TIME OF ARRIVAL ESTIMATION AND CHANNEL IDENTIFICATION IN UWB SYSTEMS

BY

MOHAMMED NASEERUDDIN MAHMOOD

A Thesis Presented to the

DEANSHIP OF GRADUATE STUDIES

KING FAHD UNIVERSITY OF PETROLEUM & MINERALS

DHAHRAN, SAUDI ARABIA

In Partial Fulfillment of the
Requirements for the Degree of

MASTER OF SCIENCE

In

TELECOMMUNICATION ENGINEERING

June 2011

KING FAHD UNIVERSITY OF PETROLEUM & MINERALS

DHAHRAN 31261, SAUDI ARABIA

DEANSHIP OF GRADUATE STUDIES

This thesis, written by **MOHAMMED NASEERUDDIN MAHMOOD** under the direction of his thesis advisor and approved by his thesis committee, has been presented to and accepted by the Dean of Graduate Studies, in partial fulfillment of the requirements for the degree of **MASTER OF SCIENCE in TELECOMMUNICATION ENGINEERING**.

Thesis Committee

Dr. Ali Hussein Muqaibel (Chairman)

Dr. Ali Al-Shaikhi
Department Chairman

Dr. Mohamed Adnan Landolsi (Co-Chairman)

Dr. Azzedine Zerguine (Member)

Dr. Salam Adel Zummo
Dean of Graduate Studies

27/7/11
Date

Dr. Tareq Al-Naffouri (Member)

Dr. Ali Al-Shaikhi (Member)

DEDICATED TO…

…MY PARENTS!

ACKNOWLEDGEMENTS

The Infinite Glory and Praise is entirely and exclusively for Allah (SWT), the Sustainer of the All that exists. He has blessed me with his bounties and bestowed me with knowledge, guidance, patience, courage and health to achieve this work. May peace and blessings be upon Prophet Mohammed (PBUH), his family and his companions.

I thank KFUPM for supporting my research besides providing me the opportunity to pursue graduate studies and letting me grow as a person rather than a just a student.

I acknowledge the support provided by the Deanship of Scientific Research at King Fahd University of Petroleum & Minerals (KFUPM) and King Abdul-Aziz City of Science and Technology (KACST) under Research Grant # NSTIP: 08-ELE44-4-1.

I deeply acknowledge with gratitude the valuable time, effort and encouragement given by my thesis advisor Dr. Ali Hussein Muqaibel. I like to thank Dr. Ali for being so patient with me throughout my research. I am grateful to Dr. Adnan Landolsi, my co-advisor, for his constructive guidance, valuable time and effort. My thesis committee consisting of Dr. Azzedine Zerguine, Dr. Tareq Al-Naffouri and Dr. Ali Al-Shaikhi has been very helpful in improving my proposal and dissertation. I am indebted to them for sharing their time and expertise.

I thank Dr. Zahid Ali Khan for being helpful and supportive.

I'd like to thank Dr. Abdullah Al-Ahmari and Mr. Umar Johar for their rectifications and suggestions during my work.

Special thanks to my seniors and colleagues at KFUPM for their valuable guidance and support and juniors for their joyful company during my research.

Above all, I thank my parents and my family members for their continuous love, encouragement, prayers, emotional and moral support throughout my life. Words fall short in expressing my gratitude towards them. A prayer is the simplest way I can repay them – 'May Allah (SWT) give them good health and give me ample opportunity to be of service to them throughout my life'.

Table of Contents

LIST OF TABLES

LIST OF FIGURES

ABSTRACT (ENGLISH)

Name : Mohammed Naseeruddin Mahmood.

Title : Time of Arrival Estimation and Channel Identification in UWB Systems.

Major : Telecom Engineering.

Date : May, 2011.

This research develops an improved time of arrival estimation for UWB systems based on Unscented Kalman Filtering (UKF). It also implements channel classification into LOS/NLOS based on parametric analysis. Accurate time of arrival estimation and correct channel identification find many applications in UWB positioning and communications.

The impact of SNR levels and fading parameters on the performance of time delay and amplitude tracking is studied for a multi tap channel. The error in estimating the time of arrival of first path is evaluated and is found to have a Gaussian behavior irrespective of the signal level and fading environment.

The Channel Impulse Response, for both simulation and experimental measurement data, is examined and the parameters Kurtosis, the Peak to Lead delay, Mean Excess delay and RMS delay spread are evaluated to classify the signals as LOS/NLOS. Also the impact of noise thresholding, deconvolution, and subsetting on classification is studied.

On the basis of the investigation carried and the results obtained, a hybrid (improved) technique for time acquisition and channel identification is proposed and a comparison of the performance with existing techniques is carried out.

MASTER OF SCIENCE DEGREE

KING FAHD UNIVERSITY OF PETROLEUM & MINERALS

Dhahran, Saudi Arabia

ABSTRACT (ARABIC)

الاسم : محمد نصير الدين محمود

العنوان : تقدير وقت وصول وتحديد قناة في نظم UWB

التخصص: الهندسة الكهربائية

تاريخ : ما يو

يكشف هذا البحث عن تقنية مطورلتقديروقت وصول الإشارات في أنظمة النطاق فائق العرض (ن.ف.ع) مبنية على ترشيح كالمن أنسينتيد (ت. ك. أ). كما أنه يصنف القناة إلى خظ النظر المباشر (مباشرة)، و غير المباشر بنائاءا على تحليل المعطيات.

ويُوجد التقدير الدقيق لوقت وصول الإشارات والتعريف الصحيح للقناة العديد من التطبيقات في أنظمة الاتصال بتقنية (ن.ف.ع) وفي تحديد الأماكن.

ولقد تم دراسة تأثير مستوى نسبة التشويش إلى نسبة الإشارة وتأثير عوامل التضاؤل على أداء تأخر وقت الوصول و تتبع قوة الإشارة على قناة متعددة المسارات.

وقيم الخطأ في تقدير وقت الوصول لأول مسار، ووجد أن لديه أداء جاوسي بخلاف مستوى الإشارة و بيئة التضاؤل.

وتم فحص استجابة القناة النبضي للبيانات المقاسة عمليا وللبيانات المحاكاة. وقيوموا بنائا على عوامل كارتوزيز و نسبة القمة إلى تأخر الطليعة و متوسط الفائض المتأخر و متوسط الجذر التربيعي للتعريض المتأخر، وذلك لتصنيف الإشارة كمباشرة وغير مباشرة. وأيضا درس تأثير قمع التشويش وطريقة الفصل و تقليل الوضع على التصنيف.

ولقد تم الحصول على نتائج بناءا على استقصاء، فاقترح أسلوب لاكتساب الوقت وتعريف القناة. و نُفذت مقارنة للأداء مع أساليب سابقة.

درجة الماجستير في العلوم

جامعة الملك فهد للبترول و المعادن

الظهران المملكة العربية السعودية

Chapter1

INTRODUCTION

1.1 Introduction and Motivation

Accurate Time of Arrival (TOA) estimation based on the received signal is the key aspect for precise ranging and synchronization of radar and communication systems. TOA estimation is a challenging issue due to noise and channel impairments. In dense multipath channels, the first path is often not the strongest, making the estimation of the TOA a difficult task [Yu04].

At the same time Non Line of Sight (NLOS) channels are one of the major obstacles for accurate ranging and localization. Hence NLOS identification and mitigation carries significant importance in wireless positioning systems.

The estimation of TOA, the identification and mitigation of NLOS errors directly improve the accuracy of the application in which they are applied such as high resolution positioning systems and synchronization.

Assuming a coarse timing estimate is already available, the focus of this research is to get a fine estimate of the time of arrival of the received signal utilizing the relatively new Ultra Wideband (UWB) Technology.

Any signal that has an absolute bandwidth of at least 500 MHz or a fractional bandwidth, i.e. ratio of difference in 3dB frequencies to the center frequency, of larger than 20% is characterized as UWB signal [Ben06]. Since these signals have very large bandwidths, compared to those of conventional narrowband/wideband signals, they have narrow time-domain pulse which means that they offer the possibility for very high positioning accuracy.

UWB systems are excellent candidates for high resolution positioning and short distance high data rate wireless applications. They have a number of features such as (i) low complexity and cost; (ii) a noise-like signal spectrum; (iii) resistance to severe multipath and jamming; (iv) a very good time-domain resolution allowing for location and tracking applications, which make it attractive for consumer communications systems.

For radiolocation applications, the most widely used positioning approach is based on TOA or Time Difference of Arrival (TDOA) data. This is because the timing information is usually extracted for synchronization purposes, and hence doesn't require additional hardware compared to Angle of Arrival (AOA) based techniques, which require more complex hardware processing. The time-based techniques are also found to be more robust in the severely distorted and multipath-impaired wireless propagation channels.

In the case of UWB signals, the additional advantage of fine timing resolution enables the receivers to resolve more closely spaced multipath components (MPCs) and improve the accuracy of the time-based positioning. Therefore TOA (or TDOA) estimation-based positioning is preferred in UWB-based positioning systems as opposed to AOA or Received Signal Strength (RSS)-based approaches.

In the remaining part of this chapter the proposed research tasks are presented followed by the literature survey.

1.2 Thesis Contribution

The objective of this research is to develop an improved time of arrival estimation for UWB systems. The objective is achieved by examining the Channel Impulse Response (CIR) and evaluating some parameters like the Kurtosis and the Peak to Lead delay and use them to refine the time of arrival estimation. Another proposed approach is based on estimating the CIR using Kalman filtering. Identifying the channel as being LOS or NLOS is directly related to the time estimation problem and hence, the performance of the above parameters is examined in classifying the channels as LOS or NLOS.

Given the non linear dependency of the channel parameters (path delays and amplitudes) on the received signals in multipath scenarios, the Unscented Kalman Filtering (UKF) approach is indeed one of the promising methods that will be investigated for the purpose of MPC parameter estimation required for efficient UWB-based positioning and NLOS mitigation.

In order to extract more information about the channel a deconvolution technique is applied since it is most needed for the characterization of wideband channels due to the limited bandwidths of available test signals as compared to the bandwidths of channels themselves. Moreover, with deconvolution the estimated channel impulse response is independent of the excitation signal, which allows us to study the effect of different pulse shapes.

Subsetting of the channel impulse response is done to evaluate the effect of sub sampling the channel profiles of the IEEE 802.15.4a channel model.

Based on the investigation carried and the results obtained an attempt to suggest a hybrid (improved) technique for time acquisition and channel identification is proposed and a comparison of the performance with existing techniques will be carried out.

1.3 Organization of the Thesis

This thesis is organized as follows. A background of related research and literature review is provided in the rest of this chapter.

Chapter 2 introduces Kalman Filtering, the Extended Kalman Filtering and their disadvantages. The advantage of applying the UKF over other filtering techniques is highlighted. An explanation of the used unscented transformation is presented along with the implemented UKF algorithm.

In Chapter 3, details about the parametric approach for LOS/NLOS classification and identification are presented. This chapter deals with the CIR and introduces the various channel statistics that were exploited in this research for channel classification.

Results obtained are presented in Chapter 4. Analysis based on the observation and discussions are covered in this section.

Chapter 5 concludes the work and presents suggestions for future work in this research direction.

1.4 Literature Survey

Due to its potential for a large number of applications there has been great interest in UWB technology in the recent years. The literature review done to assist this research

work can be classified into four areas. A large body of literature exists on the characterization of indoor propagation channels and many indoor propagation measurements were performed [Win00], [Win98], [Cas02], [Cho05a], [Cho05b] [Muq06]. UWB has good capability for short-range communications in dense multipath environments because of its fine delay resolution properties. Accurate position location is one of the most attractive capabilities of UWB technology [Dar04].

Most positioning techniques are based on the time of arrival estimation of the first path [Yu04] but in dense multipath channels generally the first path is not the strongest making the estimation of the TOA challenging.

Papers related to parametric and threshold-based TOA estimators were also reviewed.

A conventional threshold-based estimator and other algorithms implementing an ML estimator, based on a peak detection process using experimental data for TOA estimation were discussed in [Fal06]. Through analysis, it was evident that a good channel parameter estimator does not always provide noticeable gains over the conventional threshold-based estimator. A tradeoff exists between ranging accuracy, algorithm complexity, and sensitivity of the parameters' optimization to propagation conditions. If the threshold (in the *threshold-based estimator*) or the number of paths (in the *peak-detection-based estimator*) was not chosen properly, the presence of noise and multipath may lead to a biased TOA estimation even in a high SNR environment.

Threshold-based TOA estimators in dense multipath UWB channels, were discussed in [Dar08], [Dar06a], [Dar06b] wherein a comparison between Matched Filter (MF) and Energy Detector (ED) TOA estimators was made based on performance which concludes

that MF-based estimators were attractive when high ranging accuracy was desired; whereas ED-based estimators were suitable to reduce the implementation complexity and cost. Additionally, a reasonable suboptimal, but practical, choice of the threshold which uses the relationship between the probability of early detection and Threshold to Noise Ratio (TNR) was proposed and does not require a priori statistical channel knowledge. This approach was found to have a good performance in terms of MSE.

Performance investigation of various practical TOA estimators for UWB ranging systems in the presence of narrowband and wideband interference and a practical TOA estimation scheme to mitigate both narrowband and wideband interference was presented in [Dar07].

[Xu08] proposed a dedicated ranging preamble used for coarse timing estimate and multipath removal at the receiver. The preamble is designed to have a good autocorrelation property so that the leading edge of the received signal can be easily identified even in the presence of noise. A threshold-based search back algorithm based on matched filter was also introduced.

TOA estimation using a UWB dual pulse was discussed in [Zha08]. Autocorrelation and threshold crossing at the receiver is used for signal detection. Impact of different thresholds and training sequences was also studied and a comparison to the existing energy detection-based method was carried out.

In [Guv05a] a normalized threshold selection technique that exploits the Kurtosis of the received signal samples was proposed for time of arrival estimation of UWB signals. The advantages of using this technique are its low sampling rates requirements and its simple

implementation. Kurtosis was used as it captures both the statistics of individual channel realizations and the SNR of the received signal, and can be computed from the received signal samples. Error gets lower with increasing Kurtosis making it a suitable parameter for threshold selection. A performance comparison between threshold crossing and maximum energy selection-based TOA estimation algorithms [Guv05b] shows that using the Kurtosis metric, estimation error can be significantly decreased compared to fixed threshold.

In [Muc09] the same parameter, Kurtosis, was used for identifying the room typology in indoor UWB environments. For the same SNR apart from distinguishing between LOS and NLOS conditions this technique was also capable of ordering the quality of the received signal in two different LOS or NLOS rooms (LOS, Quasi-LOS, high-NLOS, low-NLOS, and extreme-low-NLOS).

Other TOA estimation techniques such as the energy detection, peak detection etc. were also studied and their performance comparison with the threshold-based detectors were made.

In [Rab06a] a ML TOA estimation strategy-based on an energy detection approach utilizing a relatively long integration window was presented which offers improved estimation accuracy whilst overcoming the practical hardware limitation associated with the need for very short integration times in the receiver. A ML estimator with partial channel state knowledge and a Generalized-ML (GML) estimator based on relatively long integration time have been proposed and later demonstrated that the GML estimator was equivalent to a sliding window-based solution [Rab06b].

TOA estimates for IR-UWB systems with different transceiver types were analyzed in [Guv06a]. The performances of TOA estimation techniques based on stored-reference, transmitted reference, and energy detection for IR-UWB systems at sub Nyquist sampling rates were analyzed. A new estimator was proposed that jointly exploits the noise statistics and power delay profile of the channel, and a Bayesian estimator was analyzed which (ideally) gives a lower bound.

[She10b] proposed a low complexity energy detection based non-coherent TOA estimation scheme. This scheme composed of two processing stages: initial signal acquisition (ISA) and fine timing estimation (FTE). To coarsely capture the arrival of the IR-UWB signals, a linear quadrature optimization (LQO)-based weighting scheme was proposed. A double-threshold test (DTT) for locating the leading edge of the IR-UWB signal being the second stage.

The issue of synchronization, due to the time sensitive nature of UWB pulse, TOA and position estimation for low complexity, low data rate UWB devices was dealt with in [Che05] wherein an evaluation of a non-coherent UWB system with positioning capability was performed.

In [Yu09] a two step TOA estimate algorithm was proposed. The first step is statistically averaging the received signals to mitigate impact of AWGN as long as possible. Using incoherent power detection algorithm, obtain rude TOA estimation which is made incoherent power detection once more in the second step so as to further optimize in time.

[Kol10] describes a method for reduction of TDOA measurement errors in UWB edge detection receivers. It presents necessary receiver modifications and an algorithm for TDOA value correction.

In [Sha10] a joint estimator of TOA and average power delay profile (APDP) was presented. First a parametric approach was assumed for the APDP, thereby assuming absence of knowledge about the APDP a priori, from which the TOA estimate was derived. The parameters for the APDP were evaluated using the least squares method. At high SNRs this technique was found to outperform the conventional techniques.

[She10a] proposed two novel methods, constant false alarm rate method and maximum probability of detection method, for TOA estimation in dense multipath and NLOS environments. Also comparisons were made with other well known schemes present in literature.

TOA estimation in the presence of pulse overlap was mentioned in [Van10]. This was achieved by a low complexity algorithm which estimates not only the first arriving path but also the rest of the channel path to have an accurate TOA estimate. The algorithm tracks the strongest few required paths by looking for the paths that are closest in Euclidean distance to the received signal.

[Ian82] examines the estimate of the difference in time of arrival of a common random for both small and large estimation errors. Experimental verifications of the approximate theoretical results were presented. The variance of the time delay estimate for both a gated mode and an ungated mode was examined and this observed variance was compared with the theoretical variance based on a small error analysis for both modes.

The Cramer Rao Lower bounds for the time delay estimation of UWB signals was presented in [Zha04] for single pulse systems and time hopping systems in AWGN and multipath channels. These synchronization errors of different monocycles have very close influence on bit error rate. The Ziv-Zakai lower bounds for Impulse Radio (IR)-UWB, for TOA-based positioning and TDOA-based positioning error, based on geometry of indoor environments were derived in [Zha10].

Literature related to the Kalman Filtering framework was surveyed. These consisted of papers dealing with Kalman Filtering, Extended Kalman Filtering and the Unscented Kalman Filtering.

For the purpose of jointly estimating the multipath channel tap delays and gains, the use of the Kalman filter (KF) framework is a very promising approach given its ability to efficiently tackle nonlinear problems (the problem at hand is indeed highly non-linear) and produce optimum results. This general optimum filtering led to several methods for channel parameter estimation, as discussed in [Kim02]. Detectors based on the approximate linearized Extended KF (EKF) were developed in [Lak02]. Although the EKF is one of the most widely used approximate solutions for nonlinear estimation and filtering, it has some limitations since it uses linearization around the current state estimate using a first order truncation of a multidimensional Taylor series expansion. These approximations often introduce large errors which may lead to suboptimal performance and sometimes divergence of the filter [Wan01].

When the system models are highly non-linear, it is observed that the effects of the higher order terms in linearized approximations can become significant. A derivative-free

nonlinear filtering approach was developed in and termed as the Unscented Kalman filter (UKF) [Jul04]. The UKF, unlike EKF, does not explicitly approximate the nonlinear process and observation models. Rather it utilizes the true nonlinear models to obtain recursive minimum mean-square error (MMSE) estimators. The state distribution is defined using a minimal set of sample points known as 'sigma points' wherein the true mean and covariance of the Gaussian Random Variable is captured, and when it is propagated through the true nonlinear system the posterior mean and covariance are accurately captured up to the 2^{nd} order for any nonlinearity [Ali09].

Chapter2

MULTIPATH CHANNEL DELAY PROFILE ESTIMATION BY THE UNSCENTED KALMAN FILTER

This chapter introduces the Kalman filtering-based approach for channel estimation. At first a general introduction to Kalman Filters and its derivates, the Extended Kalman Filter is provided followed by their disadvantages and the reason for adopting the Unscented Kalman filter. Next the UKF is explained along with the unscented transformation and the algorithm implemented in this research work. Results and discussions for this approach are presented in the later part of the section.

2.1 The Kalman Filter and the Extended Kalman Filter

The use of the Kalman filter (KF) framework is a very promising approach when we want to estimate the multipath channel coefficients and time delays because of its ability to efficiently tackle nonlinear problems for obtaining optimum results. KF provides a recursive solution to the linear optimal filtering problem. Both stationary as well as non stationary environments are applicable. Each updated estimate of the state is computed from the previous estimate and the new input data, so only the previous estimate requires storage. Apart from eliminating the need for storing the entire past observed data, KF is

computationally more efficient than computing the estimate directly, at each step of the filtering process, from the entire past observed data. The basic Kalman filter is limited to a linear assumption. More complex systems, however, can be nonlinear.

An improved form of the KF applicable to the nonlinear problems is the Extended KF (EKF). It uses linearization of the system and observation equations about the current state estimate based on a first-order truncation of a multidimensional Taylor series expansion. It assumes that the apriori distribution of the variable is Gaussian, and uses the Kalman filter framework for obtaining the estimates for the state and covariance of these estimates. The current state estimate is chosen as the best estimate, i.e.: the approximation of the conditional mean.

Even though the EKF is one of the most widely used approximate solutions for nonlinear estimation and filtering, its estimation using a first-order truncation of the multidimensional Taylor series expansion results in some limitations. This is because these approximations are valid only if all the higher order derivatives of the nonlinear function are effectively zero. In other words, it requires the zeroth and first order terms to dominate the rest of the terms. As a result, this has large implications on the accuracy and consistency of the resulting EKF algorithm. These approximations often introduce large errors in the EKF calculated posterior mean and covariance of the transformed Gaussian random variable, which may lead to suboptimal performance and sometimes the divergence of the filter.

The solution to these issues, the UKF, is presented in the next section.

2.2 The Unscented Kalman Filter

The Unscented KF (UKF) is a derivative free non linear approach that is applicable to system models that are highly nonlinear where the effects of the higher order terms in linearized approximations can become significant. The UKF utilizes the true nonlinear models to obtain recursive minimum mean-square error (MMSE) estimators. The state distribution is approximated as Gaussian, and is represented using a minimal set of carefully chosen sample points. These sample points completely capture the true mean and covariance of the Gaussian random variable, and, when propagated through the true nonlinear system, captures the posterior mean and covariance accurately to second order (Taylor series expansion) for any nonlinearity [Caf00], [Jul04], [Hay01].

We now consider the application of the UKF to our multipath channel estimation problem. We have the following nonlinear system model for an *M* multipath received signal of the form

$$h(l) = \sum_{i=1}^{M} c_i\,(l) d_{m(l)} \delta[lT_s - (m(l)T_b) - \tau_i(l)] + n(l) \qquad (2.1)$$

where $c_i(l)$, $\tau_i(l)$ are channel coefficients and time delays of the i^{th} path sampled at time instant 'l', $d_{m(l)}$ is the m^{th} transmitted symbol, T_b is the symbol interval, $\delta(l)$ is the spreading waveform and $n(l)$ is AWGN. The state-space model representation is used where the unknown channel parameters (path delays & gains) to be estimated are given by a $2M$ vector

$$\boldsymbol{x} = [\boldsymbol{c};\ \boldsymbol{\tau}] \qquad (2.2)$$

where $\boldsymbol{c} = [c_1, c_2, c_{3\ldots}\ c_M]^T$, $\boldsymbol{\tau} = [\tau_1, \tau_2, \tau_{3\ldots}\ \tau_M]^T$. Our interest lies in evaluating this vector because these estimates can be further used for channel classification. These channel coefficients and time delays are assumed to obey a Gauss-Markov dynamic channel model hence we can write:

$$c\ (l+1)\ =\ \boldsymbol{F}_c\ c(l)\ +\ \boldsymbol{v}_c(l) \tag{2.3}$$

$$\tau\ (l+1)\ =\boldsymbol{F}_\tau\ \tau(l)\ +\ \boldsymbol{v}_\tau(l) \tag{2.4}$$

where $\boldsymbol{F}_c$ & $\boldsymbol{F}_\tau$ are M x M state transition matrices and $\boldsymbol{v}_c(l)$ & $\boldsymbol{v}_\tau(l)$ are M x 1 mutually independent Gaussian random variables.

Hence, the State Model can be written as:

$$x(l+1)\ =\ \boldsymbol{F}\ x(l) + \boldsymbol{v}(l) \tag{2.5}$$

where $\boldsymbol{F}= \begin{bmatrix} \boldsymbol{F}_c & 0 \\ 0 & \boldsymbol{F}_\tau \end{bmatrix}$ is a $2M$ x $2M$ state transition matrix and $\boldsymbol{v}(l) = \begin{bmatrix} v_c(l) \\ v_\tau(l) \end{bmatrix}$ is a $2M$ x 1 process noise vector. Therefore, the scalar measurement model, which is a nonlinear function of $x(l)$, is given as

$$y(l) =\ h(x(l)) + n(l) \tag{2.6}$$

$h(.)$ is the nonlinear transformation.[Ali09]

The UKF algorithm implemented in this work is explained next.

2.3 The UKF Algorithm

In order to estimate the state '***x***' of an '*n*' dimensional Gaussian distribution, having covariance *P*, the state distribution is defined using a minimal set of sample points known as 'sigma points' wherein the true mean and covariance of the Gaussian random variable are captured, and when it is propagated through the true nonlinear system the posterior mean and covariance are accurately captured up to the 2nd order for any nonlinearity [Ali09]. The set of sigma points is given by

$$X_0 = \bar{x} \quad i=0 \tag{2.7}$$

$$X_i = \bar{x} + \sqrt{(n+\lambda)P + Q}\ ,\ i = 1, \ldots, n \tag{2.8}$$

$$X_i = \bar{x}\ - \sqrt{(n+\lambda)P + Q}\ ,\ i = n+1, \ldots, 2n \tag{2.9}$$

where $\bar{x}$ is the mean of '***x***', $\lambda = \alpha^2(n+k) - n$ is a scaling parameter, α controls the spread of the sigma points around '***x***', k is a secondary scaling parameter, and Q is the covariance of the process noise.

Sigma points are translated using the unscented transformations wherein the sigma points of **x** are evaluated from its mean and covariance and are transformed nonlinearly to a new set of sigma points of y, the nonlinear mapping of **x**. These sigma points of **y** are then used to evaluate the posterior mean and posterior covariance of **y**.

The state prediction is evaluated using

$$X_i(l+1|l) = \boldsymbol{F}\, X_i(l|l) \tag{2.10}$$

where ***F*** is the state transition matrix.

Next the predicted state vector and predicted state covariance matrix are computed as:

$$\hat{x}(l+1|l) = \sum_{i=0}^{4M} W_i^{(m)} X_i(l+1|l) \tag{2.11}$$

$$P(l+1|l) = \sum_{i=0}^{4M} W_i^{(c)} [X_i(l+1|l) - \hat{x}(l+1|l)][X(l+1|l) - \hat{x}(l+1|l)]^T \tag{2.12}$$

where $W_i^{(m)} = \begin{cases} \frac{\lambda}{\mathrm{n}+\lambda} & \mathrm{i} = 0 \\ \frac{1}{\{2(n+\lambda)\}} & i = 1, \ldots .2n \end{cases}$

$W_i^{(c)} = \begin{cases} \frac{\lambda}{\mathrm{n}+\lambda} + (1 - \alpha^2 + \beta) & \mathrm{i} = 0 \\ \frac{1}{\{2(n+\lambda)\}} & i = 1, \ldots .2n \end{cases}$ are the weights

Now the predicted observation vector and the predicted covariance are computed:

$$Y_i(l+1|l) = h(X_i(l+1|l)) \tag{2.13}$$

$$\hat{y}(l+1|l) = \sum_{i=0}^{4M} W_i^{(m)} Y_i(l+1|l) \tag{2.14}$$

$$P_{yy}(l+1) = \sum_{i=0}^{4M} W_i^{(c)} [Y_i(l+1|l) - \hat{y}(l+1|l)][Y_i(l+1|l) - \hat{y}(l+1|l)]^T \tag{2.15}$$

h(.) being the nonlinear function; and the innovation covariance is given as

$$P_{vv}(l+1) = P_{yy}(l+1) + \sigma_n^2 \tag{2.16}$$

where $(\sigma_n)^2$ is the process noise covariance.

Then the cross covariance matrix of *x* and *y* is calculated as

$$P_{xy}(\mathrm{l}+1) = \sum_{i=0}^{4M} W_i^{(c)} [X_i(l+1|l) - \hat{x}(l+1|l)][Y(l+1|l) - \hat{y}(l+1|l)]^T \tag{2.17}$$

The Kalman gain is calculated using

$$K(l+1) = P_{xy}(l+1)(P_{vv}(l+1)) - 1 \tag{2.18}$$

Now the updated mean estimate is

$$\hat{x}(l+1) = \hat{x}(l+1|l) + K(l+1)v(l+1) \tag{2.19}$$

where $v(l+1)$ is the innovation given as :

$$v(l+1) = y(l+1) - \hat{y}(l+1|l) \tag{2.20}$$

and the updated covariance is given by

$$P(l+1) = P(l+1|l) - K(l+1)P_{yy}(l+1)K^T(l+1) \tag{2.21}$$

Once the parameter estimates and the error covariance matrices are updated the process is repeated. [Ali09]

The algorithm is tabulated step by step in Table 2.1.

The UKF algorithm was successfully used in [Ali09] for multipath channel estimation with closely-spaced channels taps of CDMA signals for the purpose of mobile positioning, and we are proposing to extend this framework to UWB systems. This will assist us in developing a LOS/NLOS classification based on the estimates, apart from classification based on the true values.

STEP I: ***Sigma Points Calculation***

$X_0 = \bar{x}$ i=0

$X_i = \bar{x} + \sqrt{(n+\lambda)P + Q}\ ,\ i = 1, \ldots., n$

$X_i = \bar{x} - \sqrt{(n+\lambda)P + Q}\ ,\ i = n+1, \ldots., 2n$

$$W_i^{(m)} = \begin{cases} \frac{\lambda}{\mathrm{n}+\lambda} & i = 0 \\ \frac{1}{\{2(n+\lambda)\}} & i = 1, \ldots.2n \end{cases}$$

$$W_i^{(c)} = \begin{cases} \frac{\lambda}{\mathrm{n}+\lambda} + (1 - \alpha^2 + \beta) & \mathrm{i} = 0 \\ \frac{1}{\{2(n+\lambda)\}} & i = 1, \ldots.2n \end{cases}$$

STEP II: ***Prediction***

1. Prediction State

$X_i(l+1|l) = F\ X_i(l|l)$

$\hat{x}(l+1|l) = \sum_{i=0}^{4M} W_i^{(m)}\ X_i(l+1|l)$

$P(l+1|l) = \sum_{i=0}^{4M} W_i^{(c)}\ [X_i(l+1|l) - \hat{x}(l+1|l)][X(l+1|l) - \hat{x}(l+1|l)]^T$

2. Observation Prediction

$Y_i(l+1|l) = h(X_i(l+1|l))$

$\hat{y}(l+1|l) = \sum_{i=0}^{4M} W_i^{(m)}\ Y_i(l+1|l)$

$P_{yy}(l+1) = \sum_{i=0}^{4M} W_i^{(c)}\ [Y_i(l+1|l) - \hat{y}(l+1|l)][Y_i(l+1|l) - \hat{y}(l+1|l)]^T$

STEP III: ***Measurement Update***

1. Computing the innovation covariance and cross covariance

$P_{vv}(l+1) = P_{yy}(l+1) + \sigma_n^2$

$P_{xy}(\mathrm{l}+1) = \sum_{i=0}^{4M} W_i^{(c)}\ [X_i(l+1|l) - \hat{x}(l+1|l)][Y(l+1|l) - \hat{y}(l+1|l)]^T$

2. Calculating the Kalman gain

$K(l+1) = P_{xy}(l+1)(P_{vv}(l+1)) - 1$

3. Updating state estimation

$\hat{x}(l+1) = \hat{x}(l+1|l) + K(l+1)v(l+1)$

$v(l+1) = y(l+1) - \hat{y}(l+1|l)$

4. Updating the covariance

$P(l+1) = P(l+1|l) - K(l+1)P_{yy}(l+1)K^T(l+1)$

Table 2.1: The UKF algorithm [Ali09].

In the next section the estimation results obtained will be presented along with their interpretations. The behavior of certain parameters will be justified and other key points will be discussed.

2.4 Results and Discussions

The input to the UKF algorithm is a multipath profile with arbitrary amplitudes and time delays. The multipath channel was simulated for four paths with path spacing of half a chip. One such sample profile of four paths, with exponentially decaying average path power, is presented in Figure 2.1.

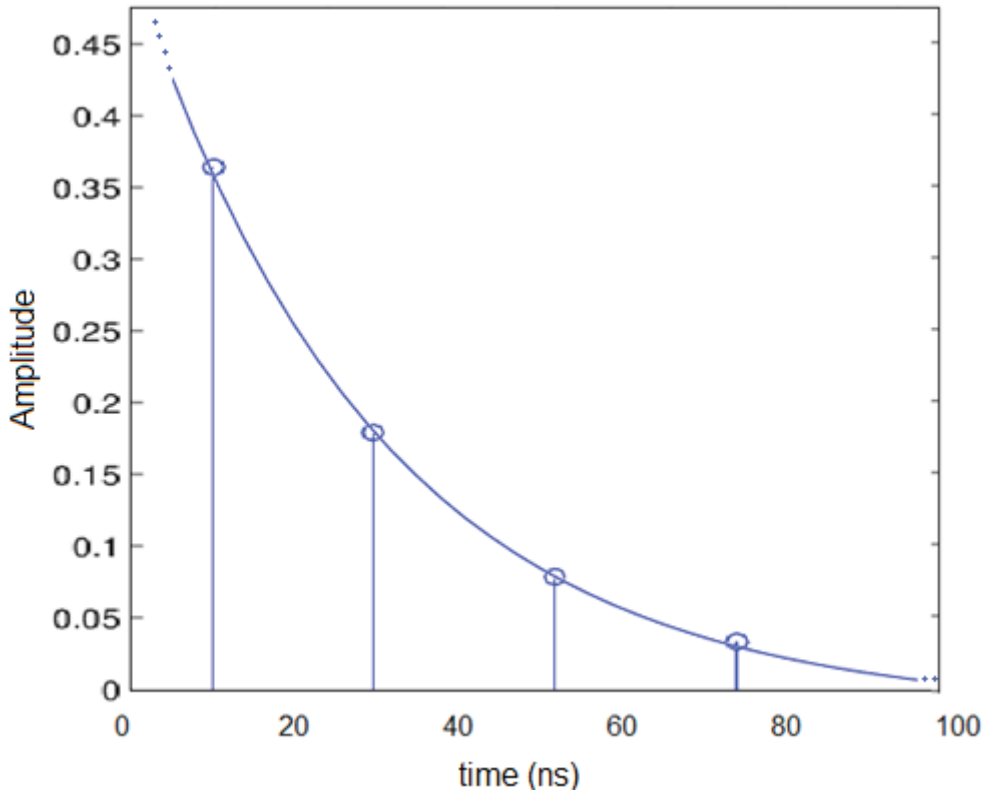

Figure 2.1: Sample multipath channel profile with exponentially decaying amplitudes.

The algorithm was implemented for 4 and 8 paths. Also the error in TOA estimation is calculated. Only the first arriving path was used in TOA error estimation. The delays have been assumed to be constant during one measurement. Time delay estimates and average amplitude estimates are plotted and from them the error in tracking is evaluated and presented in a histogram form.

A spreading sequence of length 32 with 16 symbols was transmitted. Each symbol contained 16 chips and there were 16 samples per chip. The type of fading simulated was the Nakagami fading with varying Nakagami fading parameters to study the effect of change in fading environment. The Signal to Noise Ratio (SNR) was also varied to study the effect of noise on the system performance. Two values of SNR are being reported here. The simulations are run multiple times to get a finer estimate of both the time delay and the average signal amplitude. An initial error in the time delay of up to half a chip, and an initial amplitude error of 30% are set. Both errors are assumed to be alternating in nature. An over sampled UWB waveform is selected with a pulse width of T_c, T_c being the chip duration.

It is necessary to maintain the initial error in timing within half the path spacing between two paths because if the initial error exceeds this value the algorithm is prone to divergence. However, when the initial error is less than the path spacing the UKF algorithm converges and the error is within few samples of a chip. This shows that the UKF is very sensitive to the initialization. Hence when the initial value is not close to the true delay value the steady state error is of the order of a chip or more.

The data bits, $d_{k,m}$, were not included in the estimation process, but were assumed unknown apriori. For the state space model we have taken state transition matrix to be F=0.999$I_{n\times n}$ and the process noise covariance matrix as Q=0.001$I_{n\times n}$. The scaling parameter for the UKF, κ=0, and α that controls the spread of the sigma points is set to 0.01. The other parameter β which incorporates the prior knowledge of the distribution of 'x' is maintained at 2; to capture higher order (fourth) terms in the Taylor series expansion [Ali09].

2.4.1 Time delay and Amplitude tracking

Simulations were run for various values of the Nakagami shape parameter, 'μ', and two values, μ=0.6 and 1, are being reported here. When the Nakagami shape parameter is set to 1 the channel behaves like a Rayleigh Fading channel. The SNR is varied between 5dB and 10dB. Four paths are considered with an irregular spacing between each other. Figure 2.2 shows a plot of the time delay estimates for the four paths. A SNR of 10 dB was maintained with Nakagami factor 'μ' of 0.6. It is observed that the estimates track the true value with a very good accuracy. The estimates converge after around 12 symbols and remain close to the true value after that. It was also observed that as the path power reduces the number of symbols required for convergence increase marginally.

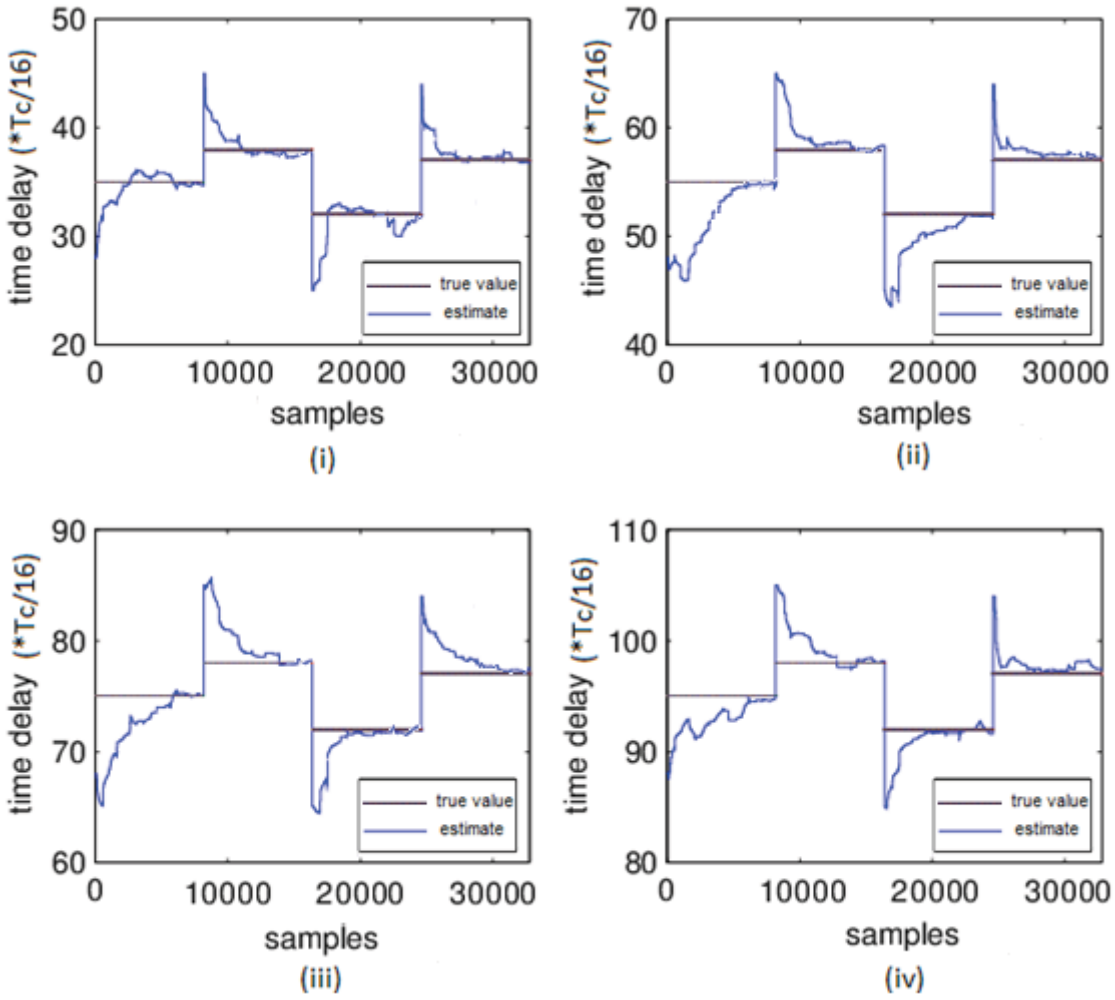

Figure 2.2: Time delay estimates for the 4 paths, SNR=10dB and μ=0.6

The average signal amplitude for the 4 paths is also estimated for the same Nakagami shaping factor and SNR value. This is presented in Figure 2.3. Close estimates of amplitude were obtained for these set of parameters.

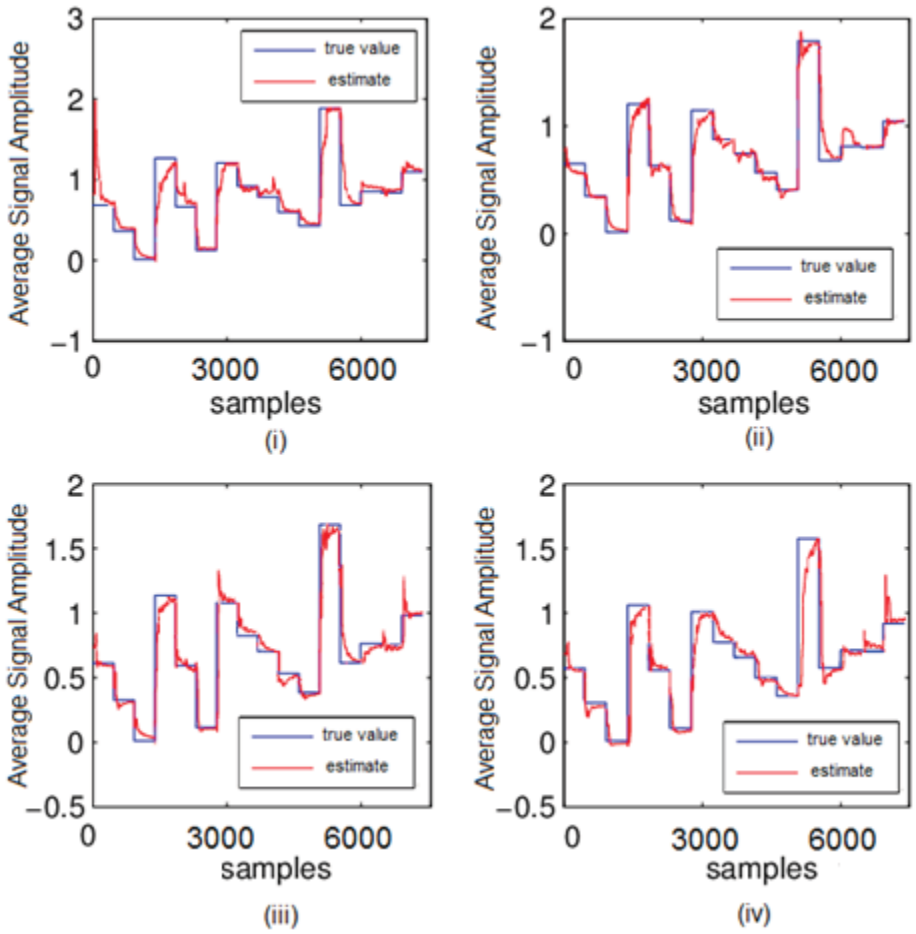

Figure 2.3: Average signal amplitude estimates for the 4 paths, SNR=10dB and μ=0.6

Figure 2.4 is a plot of the time delay estimates for the four paths. A SNR of 5 dB was maintained here with Nakagami factor 'μ' of 0.6. It is observed that with a decrease in SNR more symbols are required for convergence.

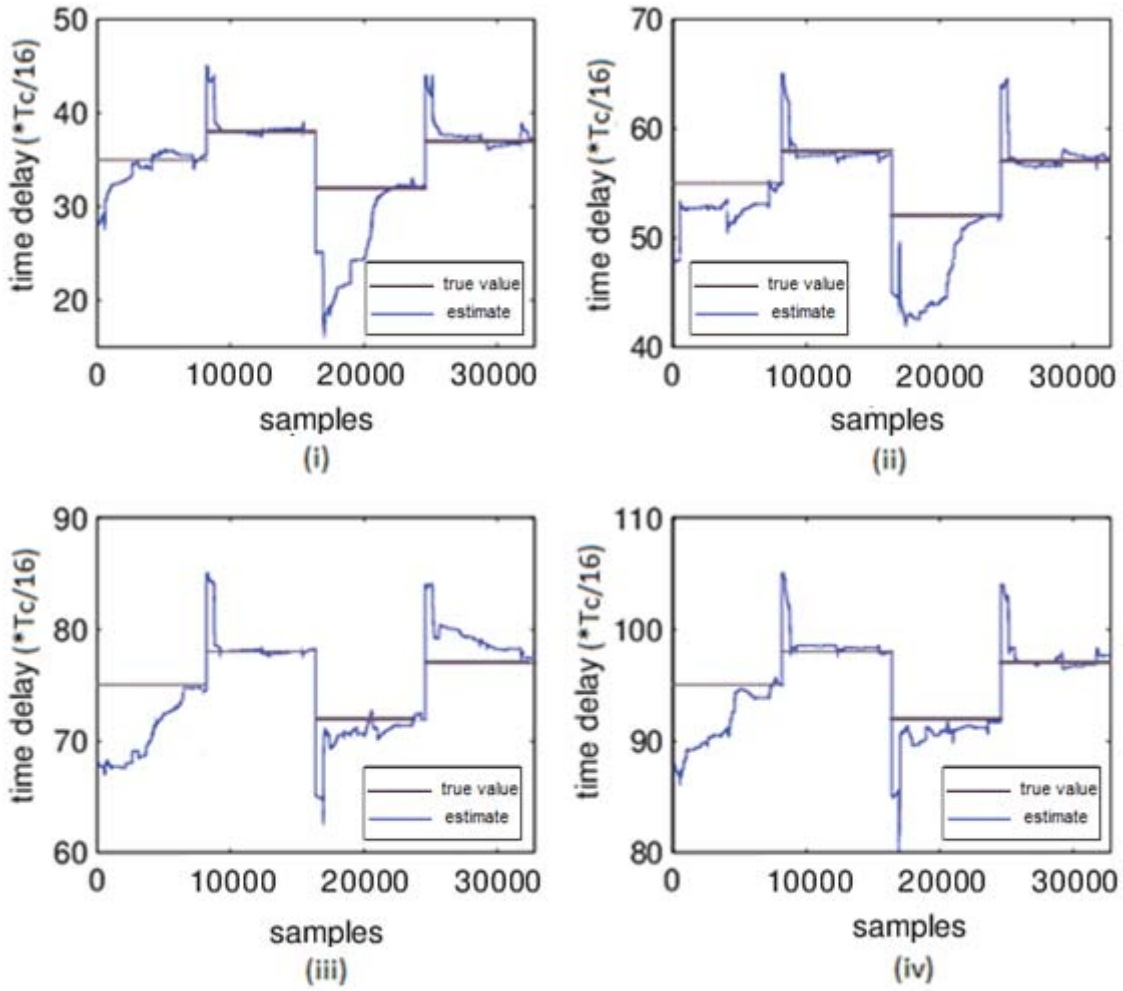

Figure 2.4: Time delay estimates for the 4 paths, SNR=5dB and μ=0.6.

The signal amplitude tracking estimates for the 4 paths for the same SNR and Nakagami factor are presented in Figure 2.5. Similar to the case for SNR of 10dB a close amplitude estimate was obtained.

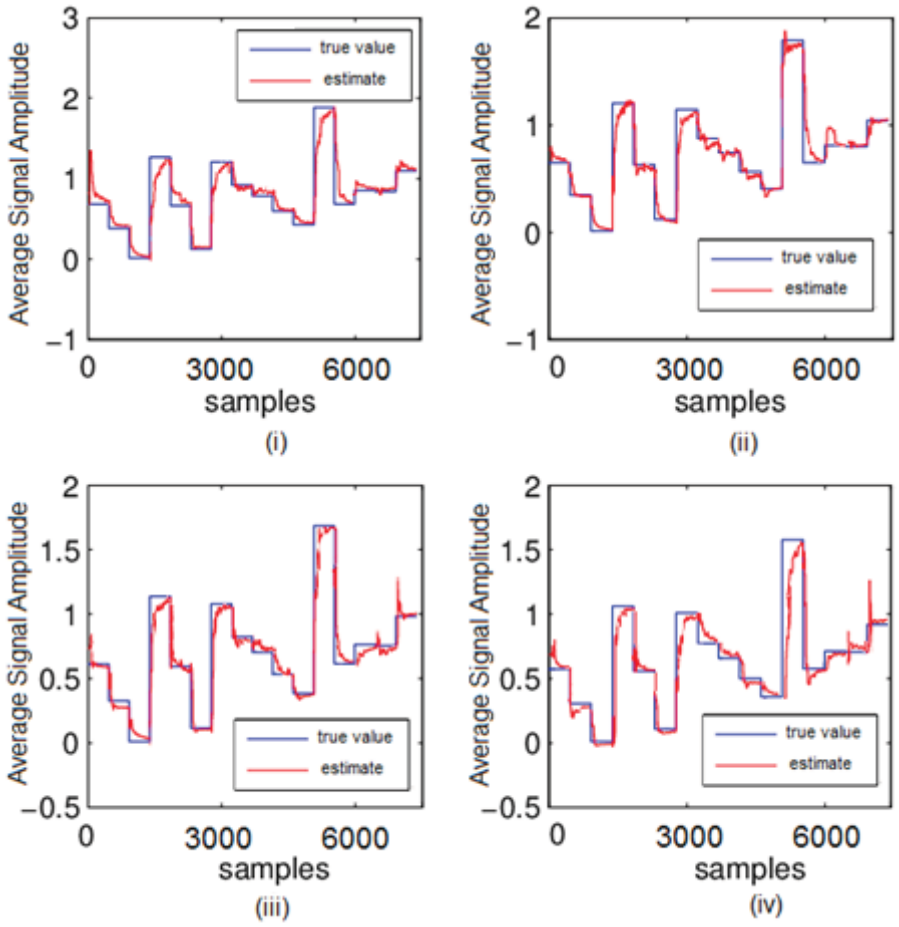

Figure 2.5: Average signal amplitude estimates for the 4 paths, SNR=5dB and μ=0.6

Figure 2.6 shows the time delay estimates for the 4 paths with a SNR of 10dB for a μ of 1.0. The estimates track quickly to the true value.

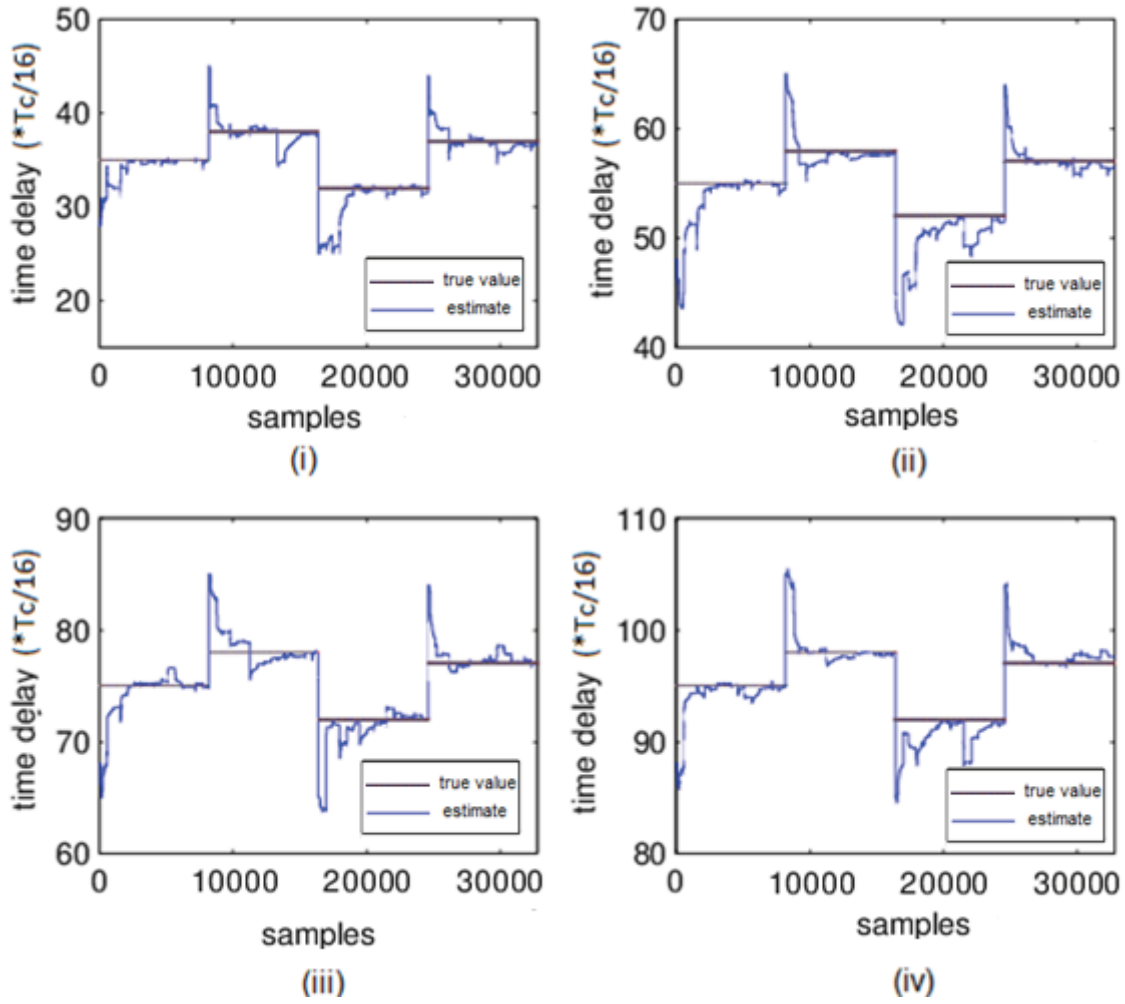

Figure 2.6: Time delay estimates for the 4 paths, SNR=10dB and μ=1.

The average signal amplitude for the 4 paths is also estimated for the same Nakagami shaping factor and SNR value. This is shown in Figure 2.7. The amplitudes are quickly tracked to the true values.

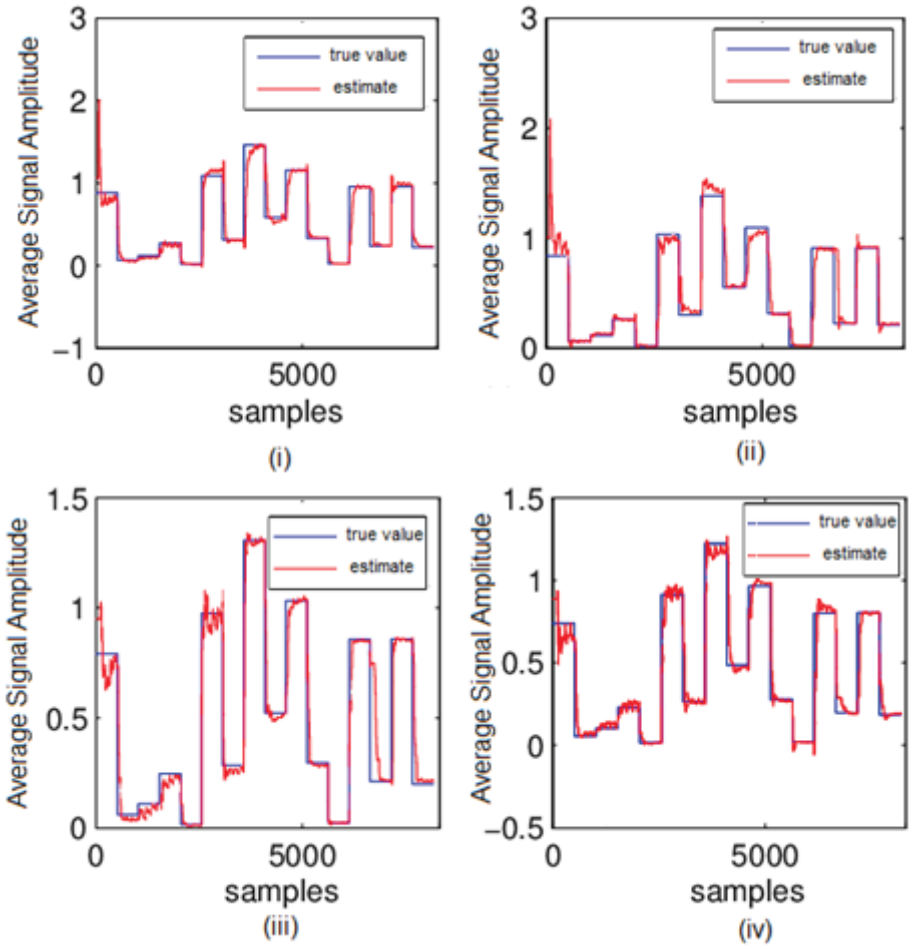

Figure 2.7: Average signal amplitude estimates for the 4 paths, SNR=10dB and μ=1.0.

Figure 2.8 is a plot of the time delay estimates for the four paths. SNR of 5dB was maintained here with Nakagami factor 'μ' of 1.0. The delays track the true values quickly with some degradation in performance compared to the case with same μ but SNR of 10dB. This degradation was observed by plotting the normalized histograms of the error in estimating the true time delay for both SNR values.

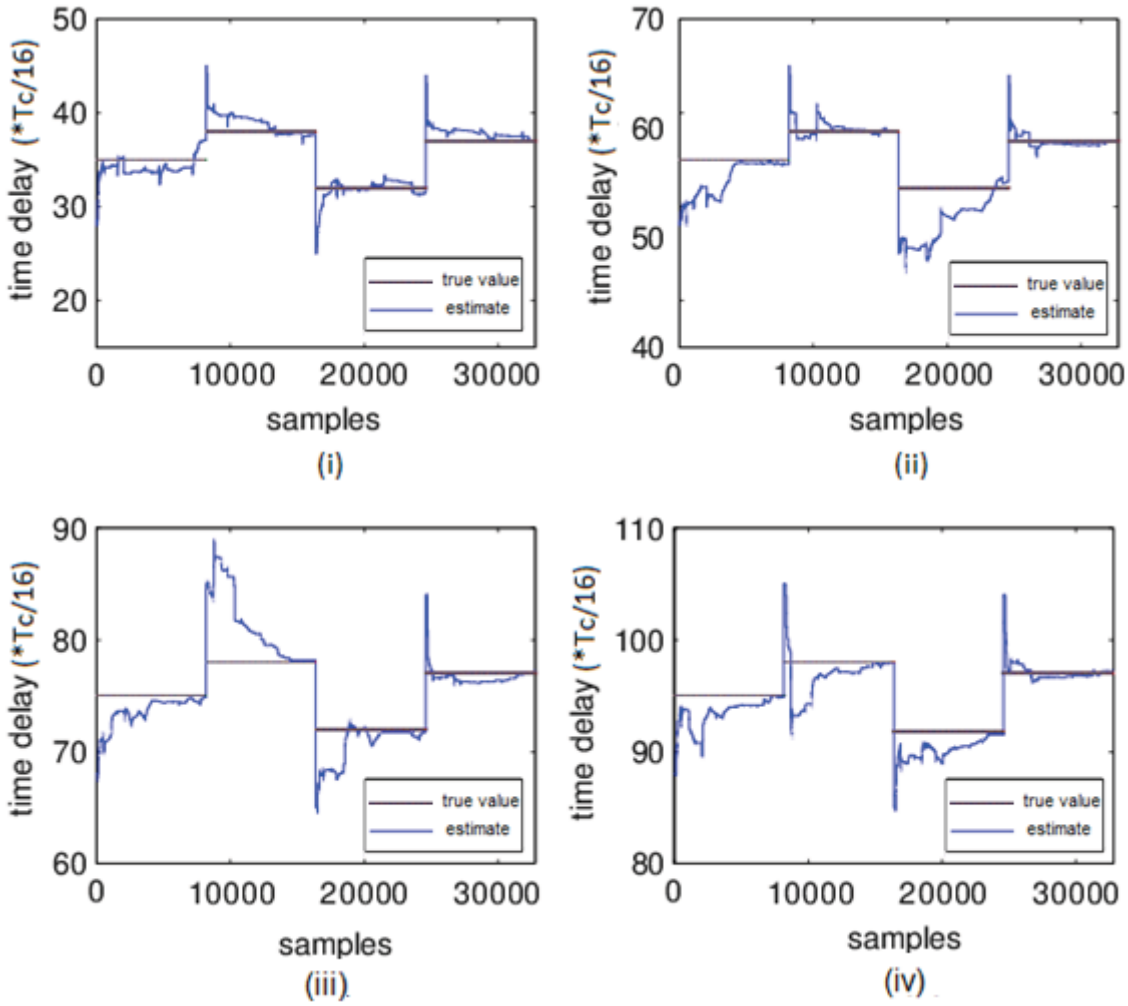

Figure 2.8: Time delay estimates for the 4 paths, SNR=5dB and μ=1.

The signal amplitude tracking estimates for the 4 paths for the same SNR and Nakagami factor are presented in Figure 2.9. The amplitudes take more samples to converge compared to when a higher SNR of 10dB was used.

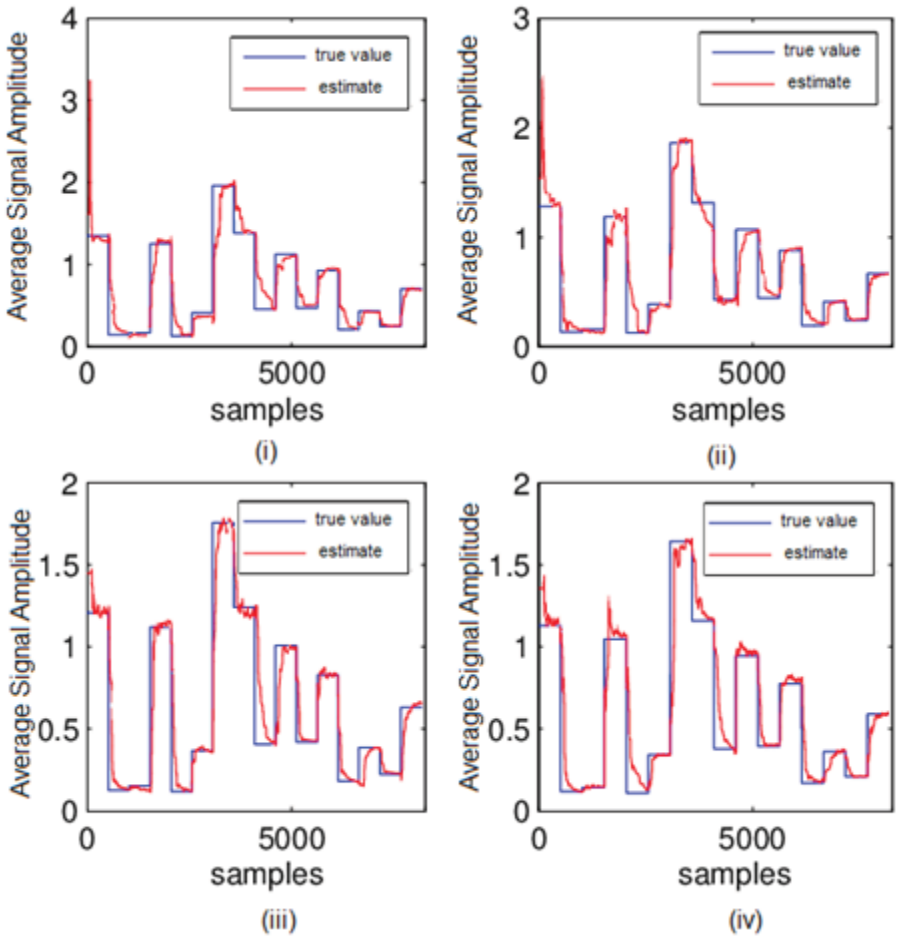

Figure 2.9: Average signal amplitude estimates for the 4 paths, SNR=5dB and μ=1.0.

Simulations were carried out similarly with number of paths increased to 8. It was observed that the number of symbols required, for the estimate to converge to the true value, are more than that compared to the 4 paths scenario. These estimates are used for developing a classification between LOS/NLOS scenarios.

2.4.2 Error Statistics in TOA Estimation

The estimation of the TOA of the first path is of most importance in mobile positioning applications. In order to do so we track the estimate with its true value. The error in tracking is calculated and plotted as a histogram. From these histograms we can evaluate

the variance in error which in turn helps in position estimation. In order to do so the error is evaluated for different fading environments and SNRs. The spacing between the paths is also altered to get generalized results. The error in estimation is evaluated for two different SNRs and two different μ values. SNR values of 10dB and 5dB were used while μ was varied between 0.6 and 1.0. The simulations were run multiple times to get consistent and averaged results. The normalized histograms of the error in TOA estimates are shown in Figure 2.10. The Gaussian distributions for the respective standard deviations, in multiples of T_c /16, are also plotted over these estimates for reference. Lower signal to noise ratios result in higher values of standard deviation, while changing the Nakagami shape parameter does not influence the standard deviation by a huge amount.

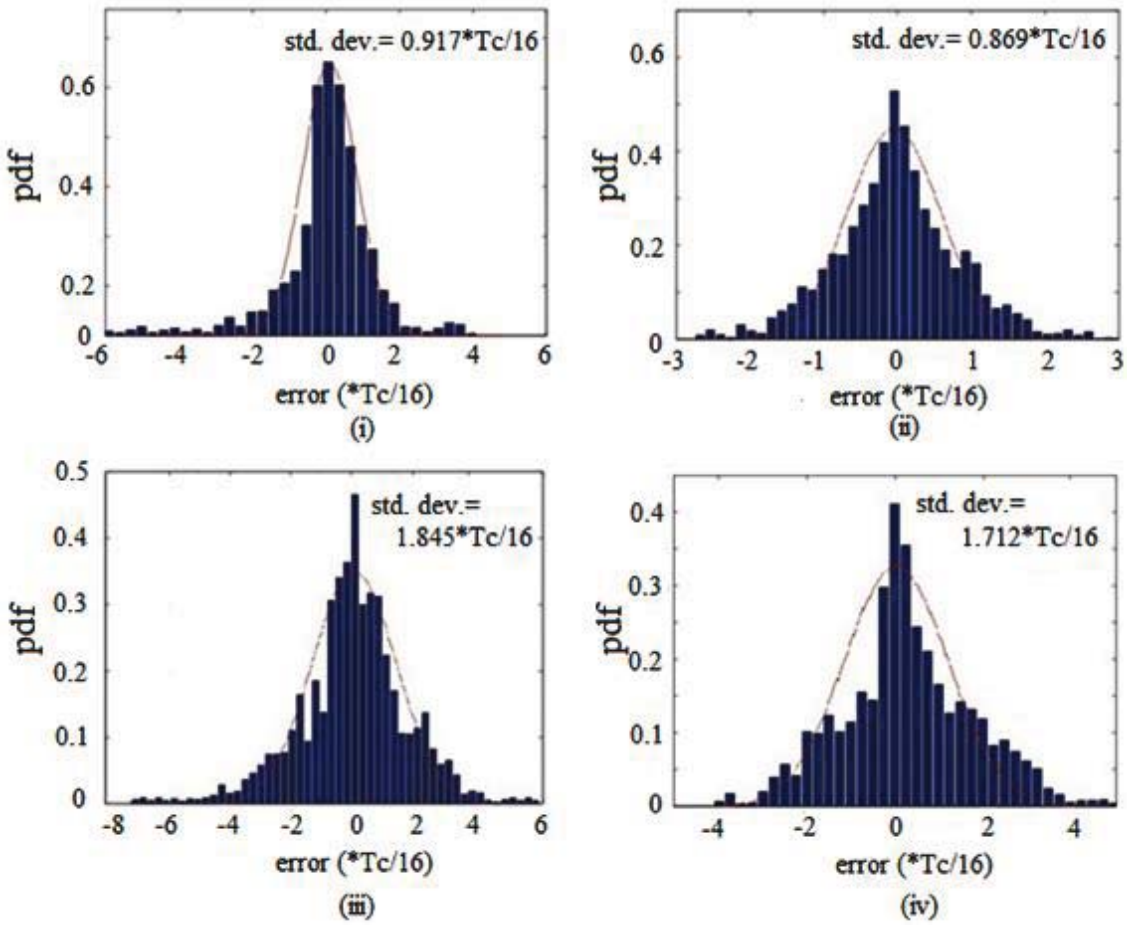

Figure 2.10: Normalized Histograms of error in TOA estimates for the first path: (i) μ=0.6, SNR=10dB (ii) μ=1, SNR=10dB, (iii) μ=0.6, SNR=5dB (iv) μ=1, SNR=5dB

This chapter has focused on the application of the UKF in UWB environment for TOA estimation. Also error in estimating the first path was studied specifically.

Experimental results of the tracking algorithm are found to corroborate the actual values for μ=1 and SNR =10dB. The algorithm is found also to have good performance when different μ values are set and this performance is directly related to the signal levels maintained. Finally the error statistics in TOA estimation were also touched upon and were found to have a Gaussian behavior.

Chapter3

PARAMETRIC APPROACH FOR CHANNEL IDENTIFICATION

A channel is completely characterized by its Channel Impulse Response (CIR). The interest in CIR measurements to develop statistical models dates back to several decades. A typical channel impulse response consists of a main response, the first arrival, followed by one or more secondary responses.

The statistical distributions of amplitudes and arrival times of these responses are sometimes used to characterize the channel. When the channel impulse response is known, a receiver can exploit the information to deliver optimum performance.

3.1 The Chanel Impulse Response and its Parameters

The CIR completely characterizes the channel. There are many partial channel characteristics such as the Kurtosis, the Peak to Lead delay, Mean Excess delay and RMS delay spread etc. as seen in Figure 3.1. These parameters not only provide intuitive measures for certain channel properties, but can also provide guidelines for the design

and evaluation of time of arrival estimation algorithms and channel identification. These parameters are studied and evaluated for different channel responses.

The Kurtosis of a certain data is the ratio of the fourth order moment of the data to the square of the second order moment (i.e., the variance) of the data. Given a channel realization *h(t)*, its Kurtosis can be calculated as:

$$k = \frac{E[(|h(t)|-\mu_{|h|})^4]}{E[(|h(t)|-\mu_{|h|})^2]^2} \tag{3.1}$$

where $\mu_{|h|}$ is the mean of *h(t)*.

Kurtosis gives a measure of whether the data are peaked or flat relative to a normal distribution; i.e., data sets with high Kurtosis tend to have a distinct peak near the mean, decline rather rapidly, and have heavy tails, while data sets with low Kurtosis tend to have a flat top near the mean rather than a sharp peak [Guv07]. Since the Kurtosis characterizes how *peaky* a sample data is, it may also be used as a tool to characterize how strong the LOS path of a certain channel is. This implies that for a CIR with high Kurtosis values, it is more likely that the received signal is LOS. Hence signals with low Kurtosis can be identified as NLOS signals and their effect can be mitigated thereby improving the timing and position accuracy. It is effective for channel classification to a great extent in most UWB environments.

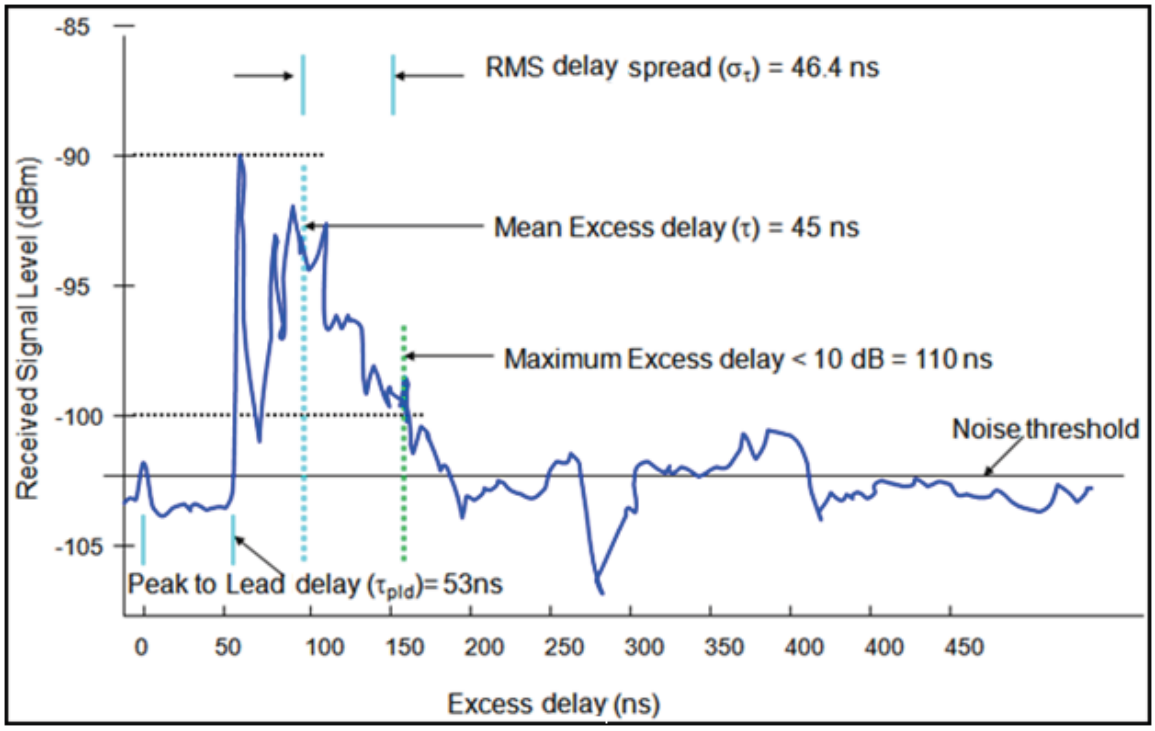

Figure 3.1: Few channel characteristics that can be used for channel identification

While the Kurtosis provides information about the amplitude statistics of the received MPCs, it does not provide any information regarding the delay properties of the received MPCs [Guv07]. This information can be achieved from the Peak to Lead delay.

The Peak to Lead delay (τ_{pld}) specifies the time interval between the first and the strongest MPCs. If the first signal path is the strongest, 'τ_{pld}=0', it is desirable TOA scenario whereas in channels that are likely to have a weaker first arrival if we select the delay corresponding to the strongest MPC as the TOA estimate then large ranging errors could appear. Selection of the noise threshold plays a major role in determining τ_{pld}. A very high value could suppress a weak LOS signal whereas a low value could result in noise terms being included as weak LOS signals, in both cases leading to error in position location. Thereby selecting an optimum noise threshold is very important. A *search-back*

algorithm can be implemented to determine the delay of the first signal component after determining the delay of the strongest MPC in order to overcome the large ranging errors [Guv06b]. The probability density function of τ_{pld} might be used to develop accurate search-back schemes. For instance, the length of the maximum search-back window can be determined.

Two other important statistics that characterize the delay information of the multipath channel are the Mean Excess delay 'τ_{med}' and the RMS delay spread 'τ_{rms}'. The Mean Excess delay and the RMS delay spread are measures of the spread of the impulse response and provide similar useful insights in identifying a channel.

The Mean Excess delay for a channel *h(t)* is given by the equation:

$$\tau_{med} = \frac{\int_{-\infty}^{\infty} t|h(t)|^2 dt}{\int_{-\infty}^{\infty} |h(t)|^2 dt} \tag{3.2}$$

and the RMS delay spread for it is calculated using:

$$\tau_{rms} = \frac{\int_{-\infty}^{\infty} (t-\tau_m)^2 |h(t)|^2 dt}{\int_{-\infty}^{\infty} |h(t)|^2 dt} \tag{3.3}$$

In narrowband systems the received signal can be approximated to the channel impulse response but this is not the case in wideband communication systems. Thus a deconvolution technique must be applied to the received signal in order to extract the impulse response of the channel. Also after deconvolution the estimated channel impulse response is independent of the excitation signal, which allows us to study the effect of different pulse shapes.

After introducing this technical background the next section discusses the methodology that was followed for conducting our research in UWB channel identification.

3.2 Methodology

In order to evaluate the mentioned proposal of parametric approach for LOS/NLOS classification, the performance will be observed via both simulation and experimental data.

To carry out the simulations, it is necessary to simulate a UWB environment and this is done using the IEEE 802.15.4a channel model. This model provides simulated impulse response for different LOS and NLOS scenarios [Mol05].

For the experimental data bank, a total of 396 channel profiles are available for channel characterization from measurements taken earlier [Muq03]. From these measurements various parameters that help in channel identification and TOA estimation will be evaluated.

3.2.1 Simulation Details: The IEEE 802.15.4a Channel Model

In order to implement the IEEE 802.15.4a channel model it is necessary to fully understand its functionality. The IEEE 802.15.4a [Mol05], based on Saleh-Valenzuela model, provides models for UWB channels operating at frequencies in the range of 2 to 10 GHz that covers indoor residential, indoor office, industrial, outdoor, and open outdoor environments (usually with a distinction between LOS and NLOS properties). A Nakagami distribution is used rather than Rayleigh distribution for the multipath gain magnitude. The model is given by

$$h(l) = \sum_{i=1}^{M} c_i(l) d_{m(l)} \delta[lT_s - (m(l)T_b) - \tau_i(l)] \quad (3.4)$$

where $c_i(l)$, $\tau_i(l)$ are complex channel coefficients and time delays of the i^{th} path sampled at time instant 'l', $d_{m(l)}$ is the m^{th} transmitted symbol, T_b is the symbol interval, $\delta(l)$ is the spreading waveform.

The model accounts for both attenuation and delay dispersion. The former subsumes both shadowing and average pathloss, while the latter describes the power delay profile (PDP) and the small-scale fading statistics; from this, other parameters such as RMS delay spread, number of multipath components carrying $x\%$ of the energy etc are derived.

The model takes into account pathloss that is not only distance dependent but also frequency dependent wherein it considers these two parameters to be independent of each other for simplicity. The frequency dependency of the antenna characteristics has to be dealt with separately though, since different proposals may have different antenna types depending on the frequency of operation and application. Also shadowing or large-scale fading which is the variation of the local mean around the pathloss is considered in calculating the pathloss.

The PDP, which is the magnitude-squared of the CIR [Sey05], gives the intensity of a signal received through a multipath channel as a function of time delay, and is computed as:

$$E\left\{\left|a_{k,l}\right|^2\right\} = \Omega_l \frac{1}{\gamma_l[(1-\beta)\lambda_1 + \beta\lambda_2 + 1]} e^{-\tau_{k,l}/\gamma_l} \quad (3.5)$$

where, $a_{k,l}$ is the tap weight of the k^{th} component of the l^{th} cluster, Ω_l is the integrated energy of the l^{th} cluster, γ_l is the intra-cluster decay time constant, and ray arrival times

are modeled as a mixture of two Poisson processes with ray arrival rates λ_1 , λ_2 and the mixture probability β.

This can be observed from Figure 3.2 which is a plot of the impulse response against time, where τ_1, τ_2, τ_3, τ_4, and τ_5 correspond to the times of occurrence of peaks of the primary and secondary responses, respectively.

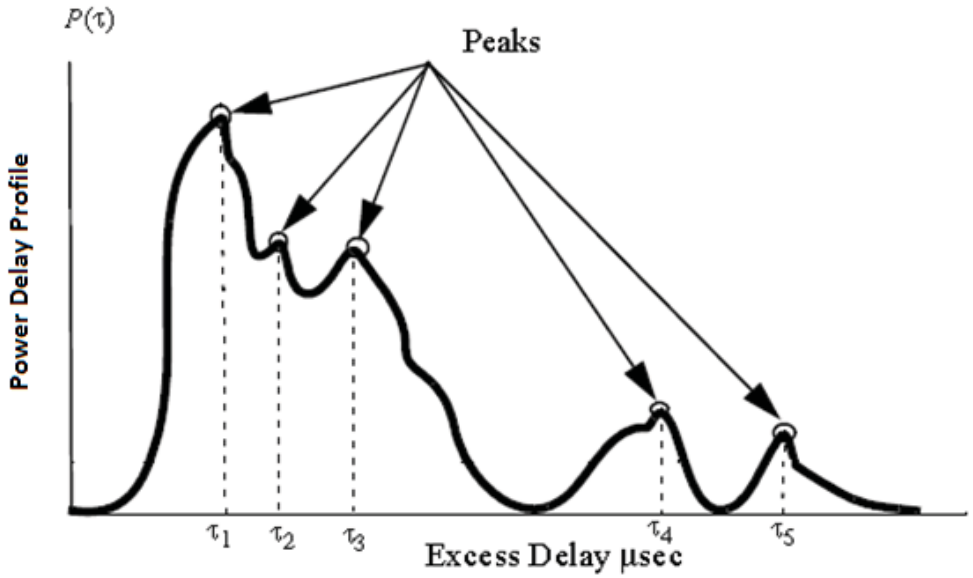

Figure 3.2: A typical Power Delay Profile

The phase is considered to be uniformly distributed and the number of clusters is considered to be Poisson distributed wherein the distributions of the cluster arrival rates are assumed to be Poisson distributed. The ray arrival times are modeled with mixtures of two Poisson processes due to the discrepancy in fitting for the different environments. The PDP is exponential within each cluster and the cluster decay rates are found to depend linearly on the arrival time of the cluster also the mean (over the cluster shadowing) mean (over the small-scale fading) energy (normalized), of the l^{th} cluster

follows in general an exponential decay. For the NLOS case of some environments, office and industrial, the shape of the PDP can be different, namely on a log-linear scale. The other parameters that are computed are the RMS delay spread, given as [Mol05]:

$$S_r = \sqrt{\left(\frac{\int_{-\infty}^{\infty} P(\tau)\tau^2 d\tau}{\int_{-\infty}^{\infty} P(\tau) d\tau}\right) - \left(\frac{\int_{-\infty}^{\infty} P(\tau)\tau d\tau}{\int_{-\infty}^{\infty} P(\tau) d\tau}\right)^2} \tag{3.6}$$

where $P(\tau)$ is the PDP, which has been used extensively in the past for the characterization of delay dispersion, the number of multipath components that is within *x* dB of the peak amplitude, or the number of MPCs that carries at least *y*% of the total energy. Since these can be determined from the PDP in conjunction with the amplitude fading statistics they are not considered a primary parameter.

The distribution of the small-scale amplitudes is considered Nakagami with a Nakagami *m*-factor of $m>0.5$ which is a lognormal distributed random variable. For the first component of each cluster, the Nakagami factor is modeled differently and it is assumed to be deterministic and independent of delay.

The code for the IEEE 802.15.4a UWB channel model was examined and analyzed. The channel impulse response corresponding to indoor residential LOS environment (CM1) is shown in Figure 3.3. Many such profiles are considered in each simulation to obtain a better estimate of the channel.

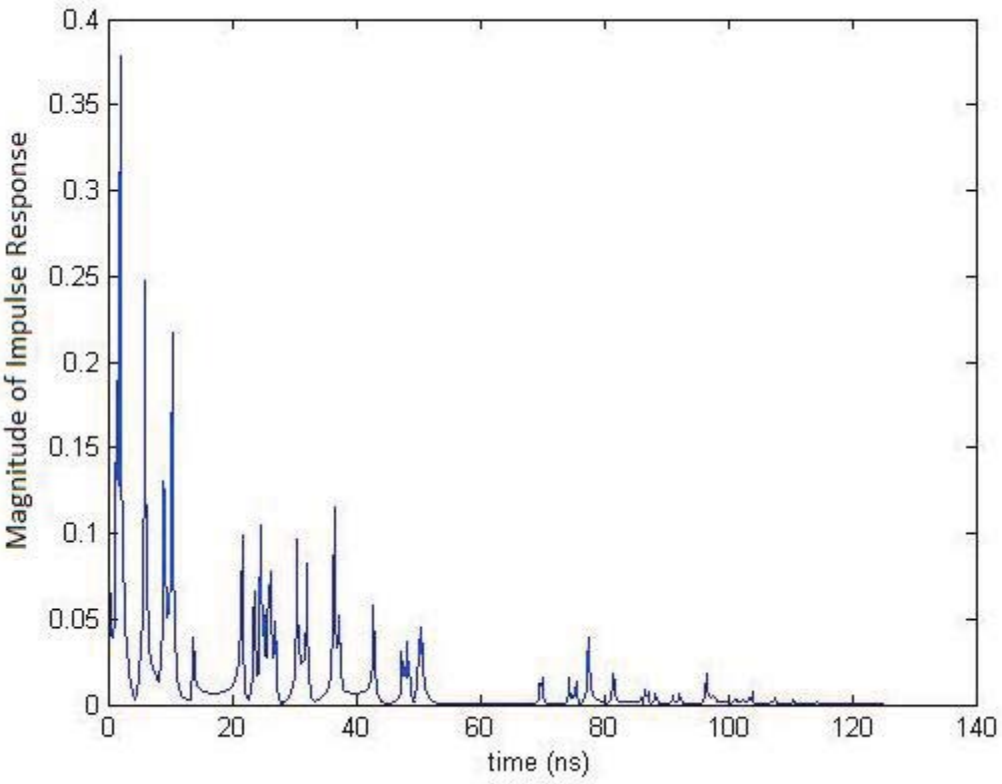

Figure 3.3: The magnitude of CIR of 1 profile of channel model 1(Indoor LOS scenario).

3.2.2 Measurement Details

In addition to simulation, we have studied the provided data bank, the measurement environment and the used parameters. To be able to use the available bank of measured CIRs, knowledge about the measurement procedure and environment is needed. The details about the measurements and their locations are briefly mentioned in this section.

The measurements were carried out in two buildings Whittemore Hall and Durham Hall on Virginia Tech Campus. Characterization of these building for some narrowband measurements and site-specific ray tracing studies has been done previously [Sei94],

[Haw91], [Rap92], [And02a], [And02b]. Thereby enabling, a comparison between narrowband and UWB channel characterization results.

The measurements were conducted in different floors at different transmitter locations and for each transmitter location measurements at different receiver locations were performed. Room-to-room, within the room and hallways are all typical indoor environments that are explored.

From the data bank one such received signal profile for the TEM antenna, which plots the received signal strength versus time duration in nanoseconds, is shown in Figure 3.4. The signal is corrupted with noise and hence it is further processed before LOS/NLOS identification can be performed. For more information about the measurements refer to [Muq03].

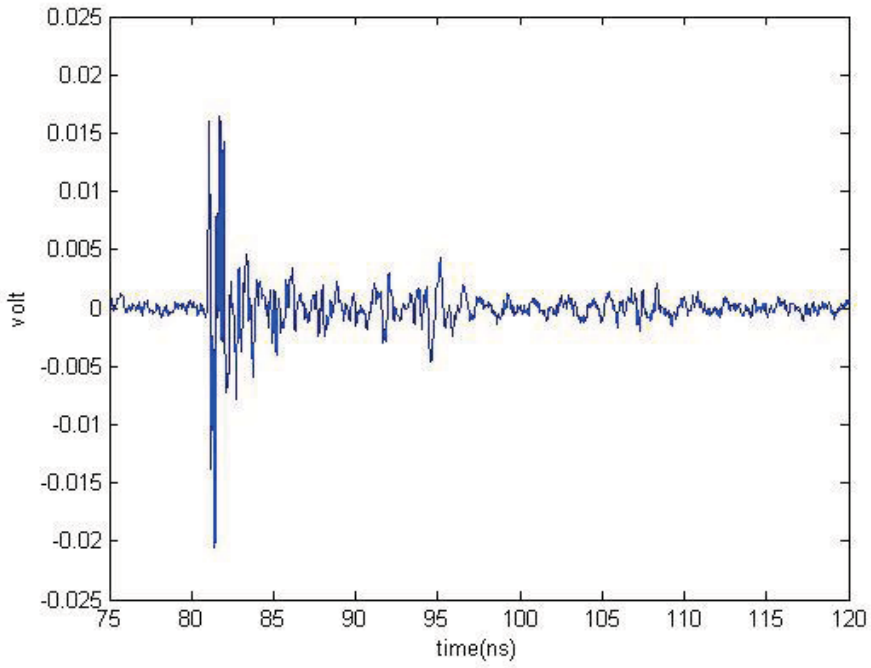

Figure 3.4: A profile of the received signal in Durham Hall for using TEM antenna

The received signal is squared, and then a threshold value is selected to limit the received signal so that unwanted noise is removed. Since measured signals can have variable propagation delay, we shift the signal such that all received signal profiles have a common time reference. The processed signal is shown in Figure 3.5. Once the signal is processed it can be used for identification purposes.

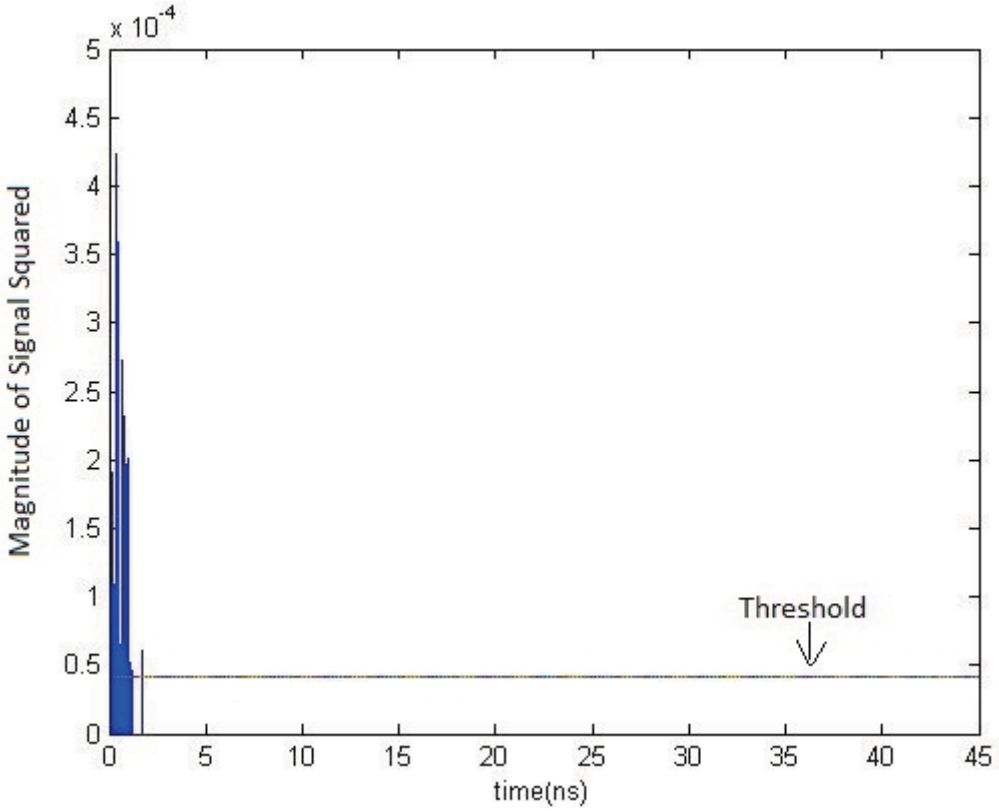

Figure 3.5: The received signal after being squared, noise removed, and shifted @ 10% threshold.

3.3 Subsetted processing of the CIR

3.3.1 Introduction

In order to reduce processing complexity and improve processing speed we propose to examine the subsetted version of the channel profile. Thus instead of using the entire channel profile for channel identification we use just a few limited paths. Thus we experiment with 5, 10 and 20 paths.

Only simulated profiles provided by the IEEE 802.15.4a channel model are used to evaluate the impact of subsetting on channel classification. 1000 channel responses are generated for each scenario. The received channel response has paths of the order of a few hundreds. We need to select a few paths from the complete profile. This can be done in three ways:

(i) either selecting the initial few paths from the full profile i.e.: selecting the first 5, 10 or 20 paths that appear in the received profile irrespective of their amplitudes

(ii) or selecting these paths uniformly throughout the profile i.e.: selecting paths spaced at regular intervals irrespective of their amplitudes

(iii) or by selecting just the peaks of each local cluster as it appears from the full profile

All of these methods have been explored via simulation.

3.3.2 Thresholding

Thresholding plays an important role in the identification process. It is done in order to remove the low amplitude noise terms that may cause an error in judgment. The selection of threshold is a crucial process. If a low value of threshold is selected high intensity noise terms could be included in our signal, on the other hand, if a high value of threshold is selected the weak received signal terms could be neglected and could thereby lead to a wrong identification.

Thresholding can be classified into two categories as depicted in Figure 3.6:

- Delay independent (DI) thresholding
- Delay Dependent (DD) thresholding

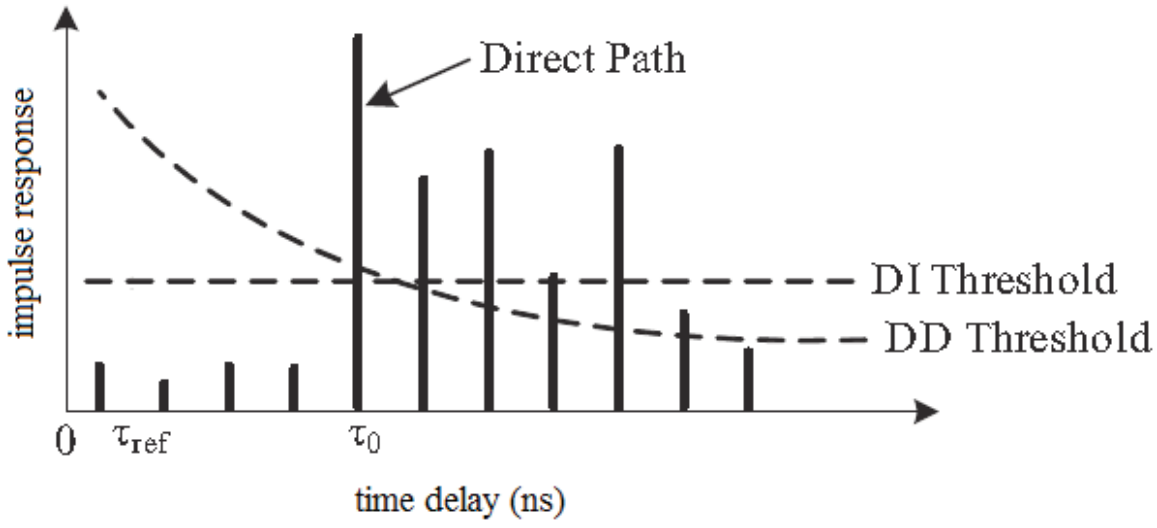

Figure 3.6: Types of thresholding

Under DD thresholding, the threshold level is dependent on the time delay of the channel profile. We have examined exponential thresholding and lognormal thresholding for both experimental and simulated data.

DI thresholding means that the threshold level is maintained constant irrespective of the delay. The threshold in this case is usually selected based on the peak signal level and noise level. In our work threshold levels of 5%, 10% and 20% of the profile maximum are studied.

Based on evaluation of the channel profiles obtained via simulation and the given measurements data it was observed that if a threshold of 10% of the maximum peak, of the profile under consideration is selected, it results in a relatively satisfactory performance.

For each LOS/NLOS scenario different cases were considered. A summary of the considered cases is given in Table 3.1.

Case #	Subsetting method	Thresholding	Objective
1	Initial samples	No thresholding	Study the effect of thresholding
2	Initial samples	10% thresholding	
3	Equally spaced spread samples	No thresholding	Study the effect of thresholding and spread sample selection
4	Equally spaced spread samples	10% thresholding	
5	Peaks of local clusters	10% thresholding	Study the effect of cluster heads

Table 3.1: Subsetting cases.

The first two cases are examined to study the impact of thresholding on the received signal. The third and fourth cases along with the previous two cases are used to study the

effect of thresholding as well as the effect of selecting the samples through different methods. In the fifth case, paths that are the local maximas in each cluster are selected.

Once the received signal is processed, the Kurtosis, Mean Excess delay and RMS delay are calculated for each of these cases. From these parameters we plot their histogram for identification between LOS/NLOS through inspection.

3.4 Deconvolution

In narrowband systems we can approximate the received signal to the channel impulse response but this is not possible in wideband systems. Thus a deconvolution technique, for classification improvement, is applied to the received signal in order to extract the impulse response of the channel. After deconvolution, the estimated channel impulse response is independent of the reference waveform, which allows us to study the effect of different pulse shapes.

In the deconvolution techniques used, the main idea was to correlate the received signal with the reference waveform and locate the correlation peaks. After locating these peaks either of the two different techniques namely Subtractive Deconvolution and Zero Forcing Deconvolution was applied. Under Subtractive Deconvolution technique, we subtract the reference waveform from the received signal at locations corresponding to the correlation peaks. In this manner once a peak was located we remove its effect on the next iteration by subtraction. An alternate approach tried was Zero Forcing wherein once the correlation peaks were located we replace the reference waveform at the corresponding locations in the received signal by zeros. For more details about the deconvolution refer [Muq09].

The received signal is a delayed and scaled version of not only one pulse shape but different pulse shapes depending on the angles of transmission and reception. Thus the received signal was deconvolved with both single and multi template reference waveforms to study the impact of using more than one template. In our case we had limited ourselves to five.

After deconvolving the received signal, its Kurtosis, Mean Excess delay, RMS delay spread and Peak to Lead delay are calculated and based on these parameters an identification is made whether the signal classifies as LOS or NLOS.

It is desired to know the minimum number of paths required for efficient classification/identification after deconvolution of the received signal. In order to do so the simulations were repeated many times by varying the number of multipaths each time and the impact on correct classification was studied each time.

3.5 Evaluation Measures

Apart from identification based on visual methods, in order to numerically evaluate the identification process, two tests were applied. These are: the Two sample Kolmogorov Smirnov (KS) test and the Likelihood Ratio test. Both these tests are explained in this section.

3.5.1 Two sample Kolmogorov Smirnov (KS) Test

The Two sample KS test is a nonparametric test used to determine if two datasets differ significantly. The Kolmogorov–Smirnov statistic quantifies a distance between the empirical distribution functions of two samples which is given by:

$$D_{12}=\boldsymbol{sup}\left(|\boldsymbol{F_1}(x)-\boldsymbol{F_2}(x)|\right) \tag{3.7}$$

where D is the distance (dissimilarity) between the input samples, *sup* is the supreme function also referred to as the Least Upper Bound, F_1 and F_2 are the empirical distribution functions of the first and the second sample respectively.

The KS test provides a parameter, 'p' value, which is a measure of the similarity between two signals. Its value ranges between 0 and 1 where 1 corresponds to identical inputs and 0 corresponds to totally different inputs.

3.5.2 Likelihood Ratio Test

After classification of the LOS/NLOS signals, a Likelihood Ratio test is developed to check if a certain received signal is correctly identified. In order to do so the knowledge of the statistics of Kurtosis 'k', Peak to lead delay 'τ_{pld}', Mean Excess delay 'τ_{med}' and RMS delay spread 'τ_{rms}' is used for hypothesis selection under the LOS and NLOS scenarios in a certain environment. From PDFs of the various parameters calculated, for a given channel realization *h(t)*, the following Likelihood Ratio tests for LOS/NLOS identification of *h(t)* are considered:

$$\frac{P_{los}^{kurtosis}(k)}{P_{nlos}^{kurtosis}(k)} \underset{H_1}{\overset{H_0}{\gtrless}} 1, \tag{3.8}$$

$$\frac{P_{los}^{pld}(\tau_{pld})}{P_{nlos}^{pld}(\tau_{pld})} \underset{H_1}{\overset{H_0}{\gtrless}} 1, \tag{3.9}$$

$$\frac{P_{los}^{med}(\tau_{med})}{P_{nlos}^{med}(\tau_{med})} \underset{H_1}{\overset{H_0}{\gtrless}} 1, \tag{3.10}$$

$$\frac{P_{los}^{rms}(\tau_{rms})}{P_{nlos}^{rms}(\tau_{rms})} \underset{H_1}{\overset{H_0}{\gtrless}} 1, \tag{3.11}$$

where $P_{los}^{kurtosis}(k)$, $P_{nlos}^{kurtosis}(k)$, $P_{los}^{pld}(\tau)$, $P_{nlos}^{pld}(\tau)$, $P_{los}^{med}(\tau)$, $P_{nlos}^{med}(\tau)$, $P_{los}^{rms}(\tau)$, $P_{nlos}^{rms}(\tau)$ are the PDFs of the Kurtosis, PLD, the Mean Excess delay spread, and the RMS delay spread corresponding to LOS and NLOS conditions, respectively. If the likelihood ratio is larger than 1, we choose the LOS hypothesis (H_0), and otherwise, we choose the NLOS hypothesis (H_1).

Rather than using the PDFs of a single parameter, we can use all of the parameters or a subgroup of them for the test. For instance, we can test a joint of two parameters at a time, which will yield for e.g.:

$$\frac{P_{los}^{joint}(k,\tau_{pld})}{P_{nlos}^{joint}(k,\tau_{pld})} \underset{H_1}{\overset{H_0}{\gtrless}} 1. \tag{3.12}$$

Since it is very difficult to obtain the joint PDFs, a suboptimal approach can be obtained by considering 'k', 'τ_{pld}', 'τ_{med}' and 'τ_{rms}' to be independent of each other resulting in

$$\frac{P_{los}^{joint}(k,\tau_{pld})}{P_{nlos}^{joint}(k,\tau_{pld})} = \frac{P_{los}^{kurtosis}(k)}{P_{nlos}^{kurtosis}(k)} \text{ x } \frac{P_{los}^{pld}(\tau_{pld})}{P_{nlos}^{pld}(\tau_{pld})} \tag{3.13}$$

For each channel realization the Likelihood Ratio test is applied, and the percentage of correctly identified scenarios is calculated. These results have been tabulated for both LOS and NLOS identification percentages using both individual and joint likelihood techniques.

Results and discussion for the parametric approach are presented in the following section.

3.6 Results and Discussions

This section summarizes the analysis results for the parametric approach in classifying the UWB channel into LOS/NLOS channels. Initially the effect of thresholding is demonstrated. In the next part, we present the PDFs for different channel parameters (Kurtosis, PLD, Mean Excess delay, RMS delay spread) for LOS and NLOS scenarios and we identify the classification threshold based on the Likelihood Ratio test. The ability to classify the channels based on these parameters is numerically evaluated using the KS test.

Since UWB signals requires large number of samples which translate into hardware cost, we evaluated the performance of the parametric analysis for classifying the channels using a subset of the channel response. A comparison between the subsetted and fully processed channel response is also presented.

Under the parametric approach LOS/NLOS classification results for both simulated environment and data available from measurements are presented.

The last part discusses the impact of extracting the parameters from the received profile as opposed to extracting them from the channel impulse response obtained through deconvolution. Numerical results from Likelihood Ratio test are presented to support the work.

3.6.1 Effect of Thresholding

It is required to filter the signal before processing. A threshold of 10% of the maximum signal peak has been set in our work. It is observed that application of a threshold to the

received waveform makes it easy to identify a LOS signal from a NLOS signal. For example, in the case of channel model CM1 (LOS scenario) and CM2 (NLOS scenario) from the PDF of the Mean Excess delay plotted for respective cases it was observed that when a threshold is applied to the received signal it makes it easier to differentiate between LOS and NLOS signals. A plot of this case is presented in Figure 3.7, which supports this argument. As seen without thresholding the PDFs overlap to a greater extent thus making classification difficult, but when thresholding is applied a demarcation can be made thereby separating the two. Similar trends were observed for other LOS/NLOS channel model pairs. Hence this threshold is maintained for the rest of the results also.

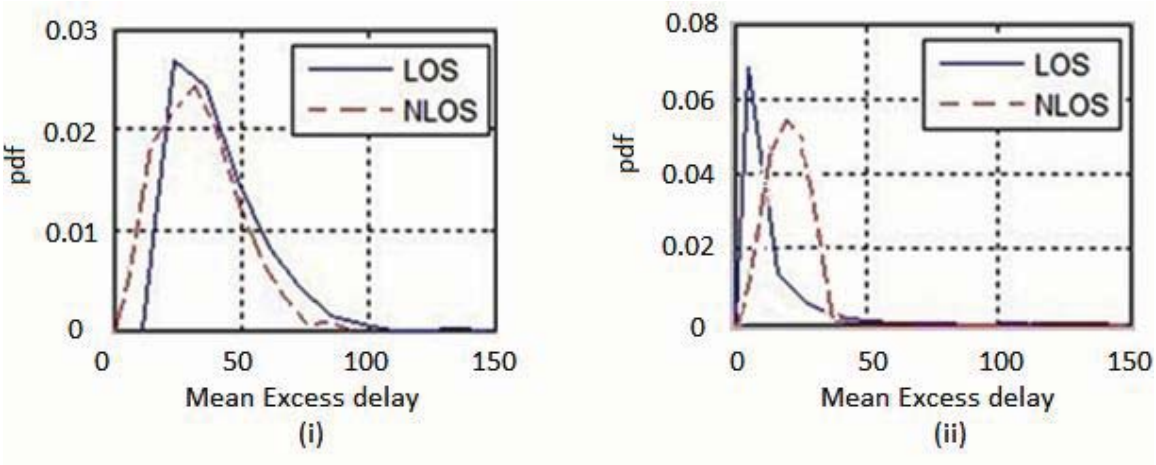

Figure 3.7: PDF of the Mean Excess delay for CM1 (LOS) & CM2 (NLOS) of the IEEE802.15.4a channel model with (i) No thresholding (ii) 10% thresholding.

3.6.2 Classifications based on Parametric Analysis

The Kurtosis, Mean Excess delay, RMS delay spread and the PLD are calculated for different environments for both LOS and NLOS scenarios. Simulated channel impulse

responses are provided by the IEEE 802.15.4a channel model. In order to ensure stable results, 1000 profiles for each LOS/NLOS scenario are generated and processed.

Based on the IEEE 802.15.4a channel model, all odd channel numbers (CM1, CM3, CM5, and CM7) belong to LOS scenarios and all even channel numbers (CM2, CM4, CM6 and CM8) belong to NLOS scenarios. CM1 & CM2 belong to indoor residential environments; CM3 & CM4 correspond to indoor office environments; CM5 & CM6 simulate outdoor environments and CM7 & CM8 resemble industrial environments [Mol05].

Figure 3.8 presents the Kurtosis of the received signals for all simulated channel models. It is observed that almost in all cases, except the case of outdoor environments, a clear classification between LOS/NLOS scenarios can be made as LOS signals tend to have a higher Kurtosis value compared to the NLOS signals. For example, for the indoor office environment CM3 & CM4 a value of 80 for the Kurtosis can be used as threshold for distinction between LOS/NLOS scenarios. Similar results were obtained by [Guv07].

Figure 3.9 shows the PLD plotted for all the channel models. It is observed that a LOS signal has a low PLD compared to NLOS signals for any given environment. From the figure, it is possible to distinguish between NLOS and LOS signals, for example, for the case of CM7 and CM8 we can say that a PLD value of 4 can be taken as a threshold and any signal with a PLD lesser than that can be classified as a LOS signal.

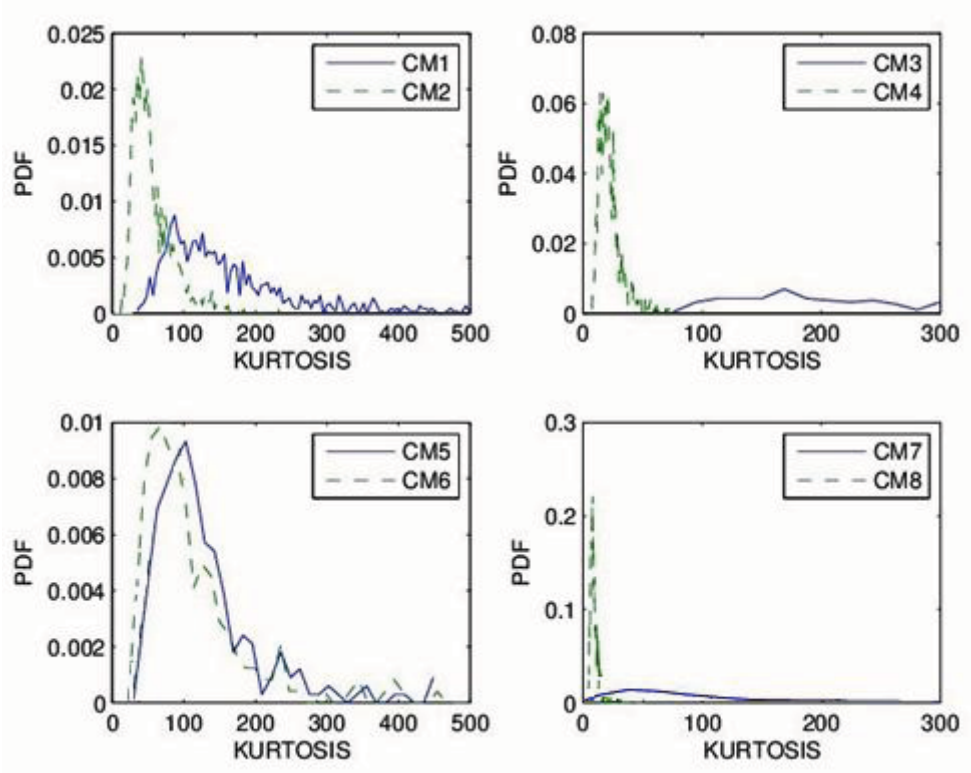

Figure 3.8: PDF of Kurtosis of IEEE 802.15.4a channel models.

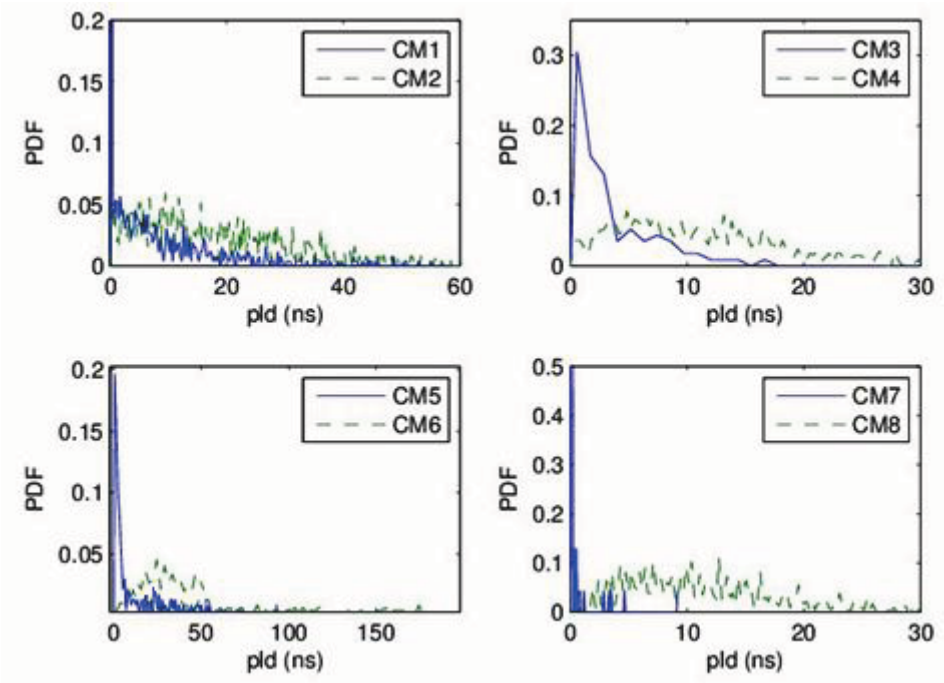

Figure 3.9: PDFs of PLD of IEEE 802.15.4a channel models.

The Mean Excess delay for all channel models is shown in Figure 3.10. A distinction between LOS/ NLOS scenarios is visible from the plot and is confirmed that LOS signals have a lesser Mean Excess delay compared to NLOS signals for a given set of scenarios. The numerical measure for the similarity or the degree of similarity/distinction between the PDF is given later.

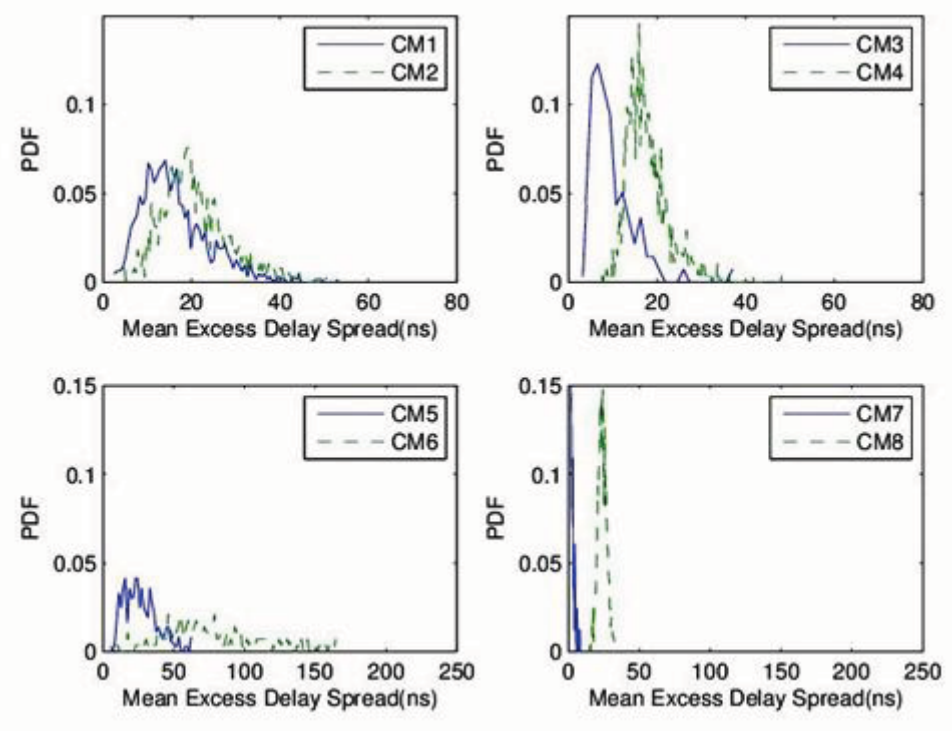

Figure 3.10: PDFs of Mean Excess delay of IEEE 802.15.4a channel models.

Also RMS delay spread for the received profiles is evaluated and plotted to assist LOS/NLOS identification. Figure 3.11 presents the PDFs of RMS delay spread of all channel models of the IEEE 802.15.4a. It also provides a fair LOS/NLOS identification opportunity.

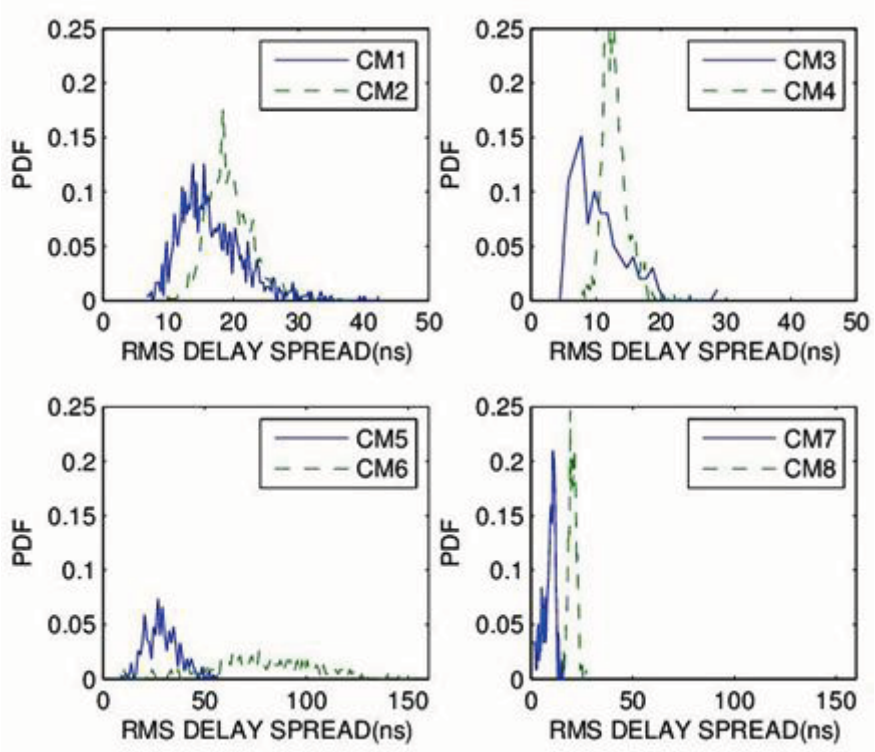

Figure 3.11: PDFs of RMS delay spread of IEEE 802.15.4a channel models.

While the Kurtosis can be a good parameter for CM3/CM4 and CM7/CM8, it is not very useful for other environments. For example, in the case of CM5/CM6, i.e. Outdoor environments, it is difficult to make a decision based on this parameter. PLD is found to be much effective in this case. A signal with a PLD of 10ns or less can be considered as LOS signal. Similar is the case with Mean Excess delay and RMS delay spread. In CM7/CM8, for example, a signal with a Mean Excess delay spread of 8ns or more can be considered as NLOS signal. RMS delay spread is found to be effective in almost all environments except CM1/CM2, where the decision is unclear.

The results of the KS test, i.e. the '*p* values', are presented for the different parameters under both LOS and NLOS conditions in Table 3.2 for the simulated IEEE 802.15.4a

channel model. The smaller the '*p* value', the more likely it is that the two signals are different.

From this table we can observe that while all parameters help in clearly distinguishing the LOS from NLOS for the Industrial environment, this is not the case with the rest of the environments. For example, in the Residential scenario only PLD gives distinguishable results. Overall it is observed that PLD performs well except for the scenario of Indoor Office (*p=0.5815*) where Kurtosis (*p=0.1862*) is found to present best results. Hence a classification using a joint decision involving more than one parameter is more efficient.

Parameters / Channel	Kurtosis	PLD	Mean Excess delay	RMS delay spread
Residential (CM1 & CM2)	0.4913	0.2609	0.9811	0.8927
Indoor Office (CM3 & CM4)	0.1862	0.5815	0.6158	0.4333
Outdoor (CM5 & CM6)	0.7864	0.2811	0.4351	0.4217
Industrial (CM7 & CM8)	0.2015	0.2132	0.1612	0.1862

Table 3.2: KS test for all profiles of the IEEE 802.15.4a channel model

The Likelihood Ratio test was also applied to both simulated and measurement profiles to check the probability of correct identification of a particular profile. These results are tabulated in Table 3.3. The higher the probability of correct identification the better is our approach. It can be seen that using individual metrics may yield high identification percentage only for certain channel models (depending on the amplitude and delay characteristics of the channel under consideration), while the joint approach involving

Kurtosis, PLD and RMS delay spread achieves best identification percentage for all the channel models. Almost all channel models could be identified with a minimum of 90% certainty for the joint optimization case.

Parameters / Channel	Kurtosis	PLD	RMS	Kurtosis & PLD	Kurtosis & RMS	PLD & RMS	Kurtosis, PLD & RMS
CM1 (LOS)	74.9	72.3	63.2	85.2	79.2	80.5	89.1
CM2 (NLOS)	80.2	70.9	73.2	87.3	89.7	81.2	91.2
CM3 (LOS)	95.1	81.3	69.2	90.2	100	89.3	94.4
CM4 (NLOS)	93.2	74.3	89.2	92.7	99.4	92.7	95.7
CM5 (LOS)	63.8	87.3	91.3	89.9	87.4	89.8	97.3
CM6 (NLOS)	69.7	78.7	84.3	83.6	81.3	81.2	92.4
CM7 (LOS)	98.3	97.3	99.7	98.6	96.9	99.0	99.1
CM8 (NLOS)	98.7	96.4	99.9	98.9	94.7	98.9	99.4

Table 3.3: LOS/NLOS identification percentages for full IEEE channel model.

All parameters are found to perform well in Industrial environment, with a minimum correct identification percentage of 98.7%, but for other environments some parameters outperform others. Apart from Industrial environments, Kurtosis was found to give good results, as close as 95.1%, for CM1/CM2 and CM3/CM4, i.e.: Residential and Indoor Office environments respectively where RMS delay spread was found to have inferior performance. RMS delay spread gave good results as close as 99.9% for CM5/CM6, i.e.:

Outdoor environments, where Kurtosis had lower identification percentage. The PLD performed moderately well irrespective of the environment, giving best identification percentages as high as 97.3%.

3.6.2.1 Performance of Parametric classification for Practical Measurements

The published results for the parametric classification were all based on simulation [Guv07]. In this section we evaluate the performance of practical measurements.

Measurements that were received were processed initially then from those processed profiles Kurtosis and other parameter were extracted. Figure 3.12 (i) presents the PDF of the Kurtosis of these measurements, Figure 3.12 (ii) presents the PDF of the PLD while Figure 3.12 (iii) is a plot of the PDF of the Mean Excess delay. Similarly the PDF of the RMS delay spread for the measured data is plotted in Figure 3.12 (iv).

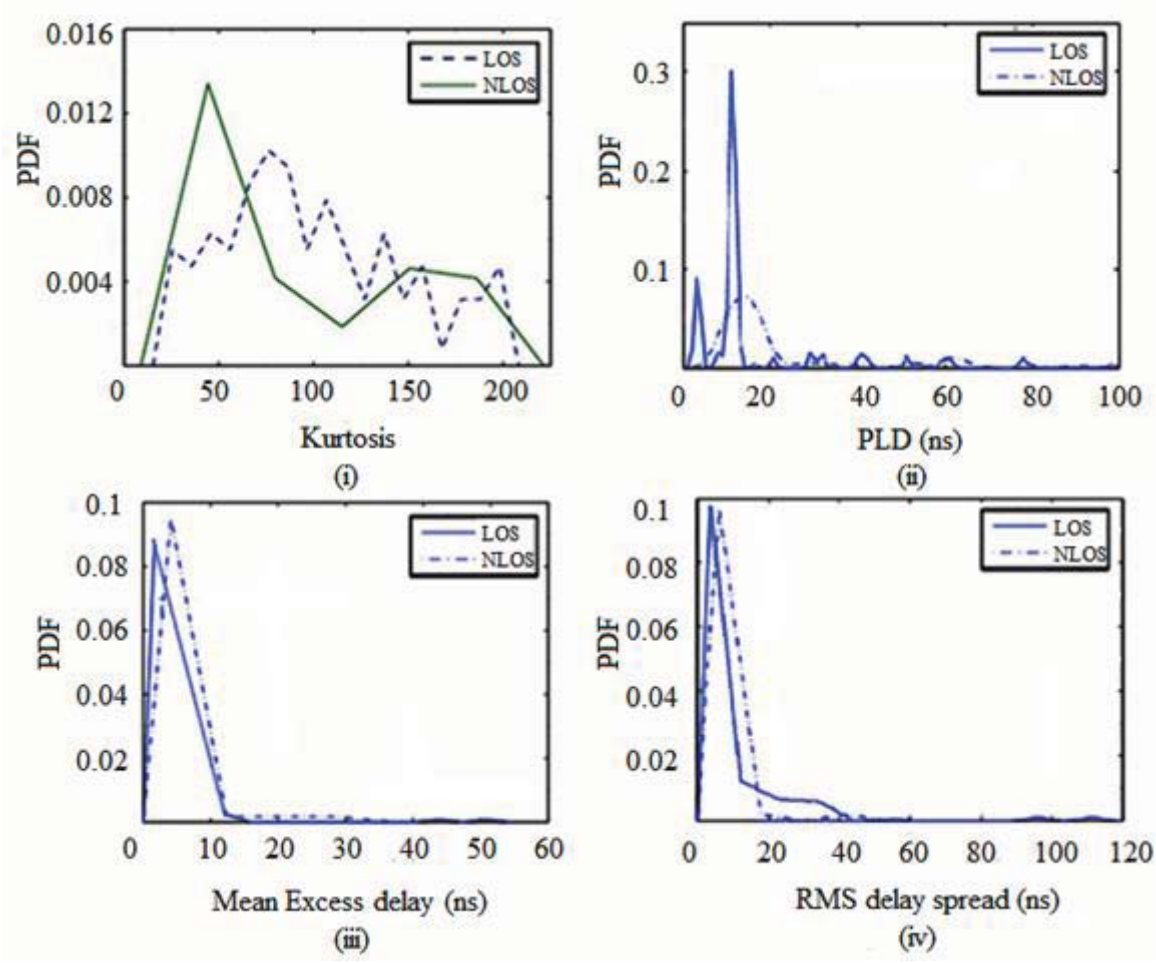

Figure 3.12: PDF of (i) Kurtosis, (ii) Peak to Lead delay, (iii) Mean Excess delay, and (iv) RMS delay spread of measurement data.

It is observed that a clear classification between the LOS/NLOS curves is not possible as the respective PDF curves are not distinct, thus a fair threshold for discrimination is not selectable.

The Likelihood Ratio test was also applied to the measurement data and is presented here in Table 3.4. Similar to the simulated profiles, it is observed that the joint approach involving Kurtosis, PLD and RMS delay spread achieves better identification percentage for all the channel models.

Parameters / Channel	Kurtosis	PLD	Mean Excess delay	RMS delay spread	Kurtosis, PLD & RMS
LOS	60.3	78.2	78.1	76.8	80.4
NLOS	77.6	68.3	80.2	79.2	82.7

Table 3.4: LOS/NLOS identification percentages for measurements pre deconvolution.

It is evident from the above analysis that the parametric classification based on the IEEE 802.15.4a is very optimistic. The experimental evaluation showed inferior results in terms of classifications. For instance the two sample KS test for the Mean Excess delay and RMS delay spread for the experimental data gives a '*p*' value of 0.92 and 0.94 respectively, which are very high and unacceptable values for classification. Hence more signal processing is required before a satisfactory classification can be made. It is suggested that deconvolution will increase the resolution of the received signal and hence could result in an improved classification.

3.6.3 Impact Classification based on Deconvolved Impulse Response

Since the received signal is the output of the channel rather that the channel impulse response itself, we deconvolve the received signal so that the effect of using different pulse shapes can be studied. Figure 3.13 shows a comparative plot of the Kurtosis plotted before deconvolution and after deconvolution of the received signal. For illustrating the impact of deconvolution, CM1 of the IEEE 802.15.4a channel model was convolved with a reference template to simulate a received signal, and later it was deconvolved.

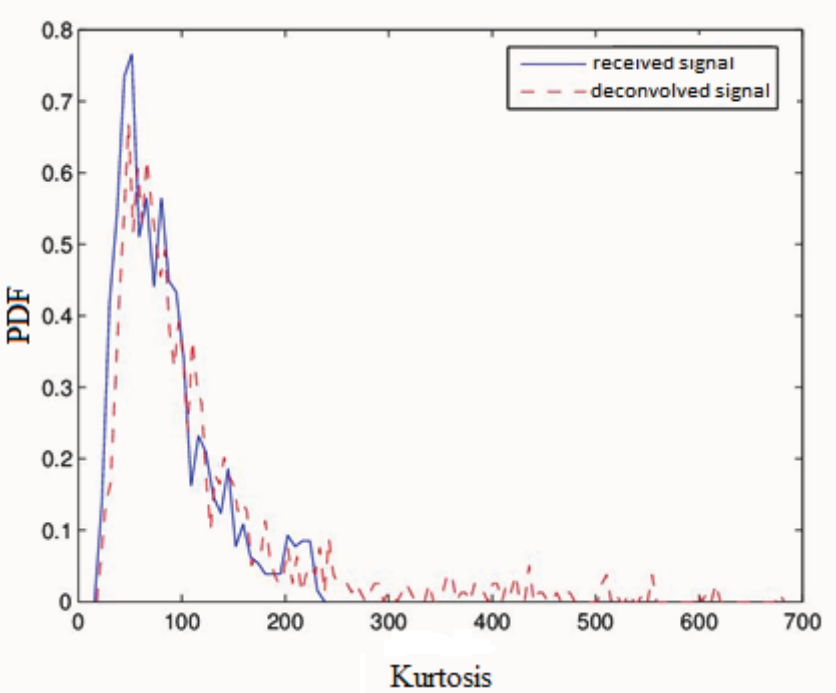

Figure 3.13: Comparison of Kurtosis (for CM1 of the IEEE 802.15.4a channel model) before and after deconvolution.

The effect of deconvolving the signal on the Kurtosis is evident from the plot. The Kurtosis value of the impulse response reduces by a small amount when convolved with a waveform due to the spread of that waveform. This deconvolution technique will be studied for the profiles from the measurement data bank, since the received signal from the measurement data bank are a convolution of the true channel impulse response and the reference input waveform.

Deconvolution was applied using both single template and multi template and was found that it was better to adopt a multi template approach rather than a single template approach since when we use a single template we tend to lose some of the significant multipath components just for the reason that they do not resemble our single template.

Both Subtractive deconvolution and Zero Forcing deconvolution techniques were implemented and was observed that the Subtractive deconvolution technique outperforms the Zero Forcing technique. One of the reason is that when two paths are closely spaced then applying a Zero Forcing deconvolution results in some residue signal that does not resemble the input waveform thereby resulting in undesired outputs. The Subtractive deconvolution on the other hand subtracts the first signal from the closely spaced received signal thereby resulting in a multipath that resembles the input template. Since closely spaced multipath signals are a significant feature of UWB systems hence subtractive deconvolution is preferred. [Muq10]

The number of successfully deconvolved multipaths also affects the performance of our analysis. It was observed that though 10 paths were sufficient to make a satisfactory classification between LOS and NLOS, a selection of 20 paths gave a reliable classification as it captured most of the possible energy of the received signal.

The energy capture is defined as [Muq10]:

$$EC = \left\{1 - \frac{||r(t) - rc(t)||^2}{||r(t)||^2}\right\} * 100\% \tag{3.14}$$

where $r(t)$ is the received signal and $rc(t)$ is the reconstructed deconvolved signal.

Figure 3.14 shows the percentage energy capture with respect to number of paths for one of the received profiles of the LOS scenario. We can observe that the percentage of captured energy when 10 multipaths are used is close to 70 if we increase the number of paths by 5 this percentage also increases by 5 till we reach 20 paths. Increasing the number of paths beyond 20 does not increase the percentage of captured energy by a

significant level. Similar trend is observed for the rest of the profiles of both LOS as well as NLOS profiles. Thus 20 multipath components were considered in our analysis.

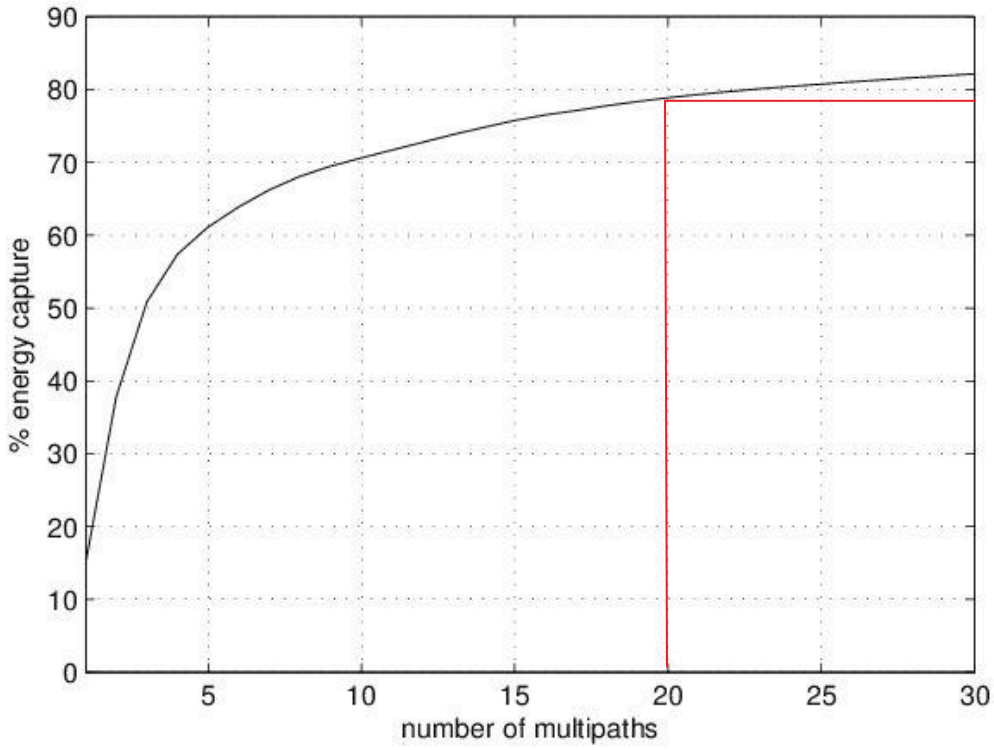

Figure 3.14: Energy captured with respect to number of deconvolved multipaths.

Figure 3.15 shows the PDFs of the Kurtosis, PLD, Mean Excess delay and RMS delay spread for the LOS and NLOS scenarios. It is obtained by considering multi template reference waveform and subtractive deconvolution. A fair classification can be made between LOS and NLOS signals based on these PDFs. LOS signals are observed to have a higher Kurtosis value as expected, whereas most of the NLOS signals tend to have a small Kurtosis value. A threshold of 60 could be considered, signals with Kurtosis values above which can be classified as LOS signals, and signals having lower Kurtosis values as NLOS.

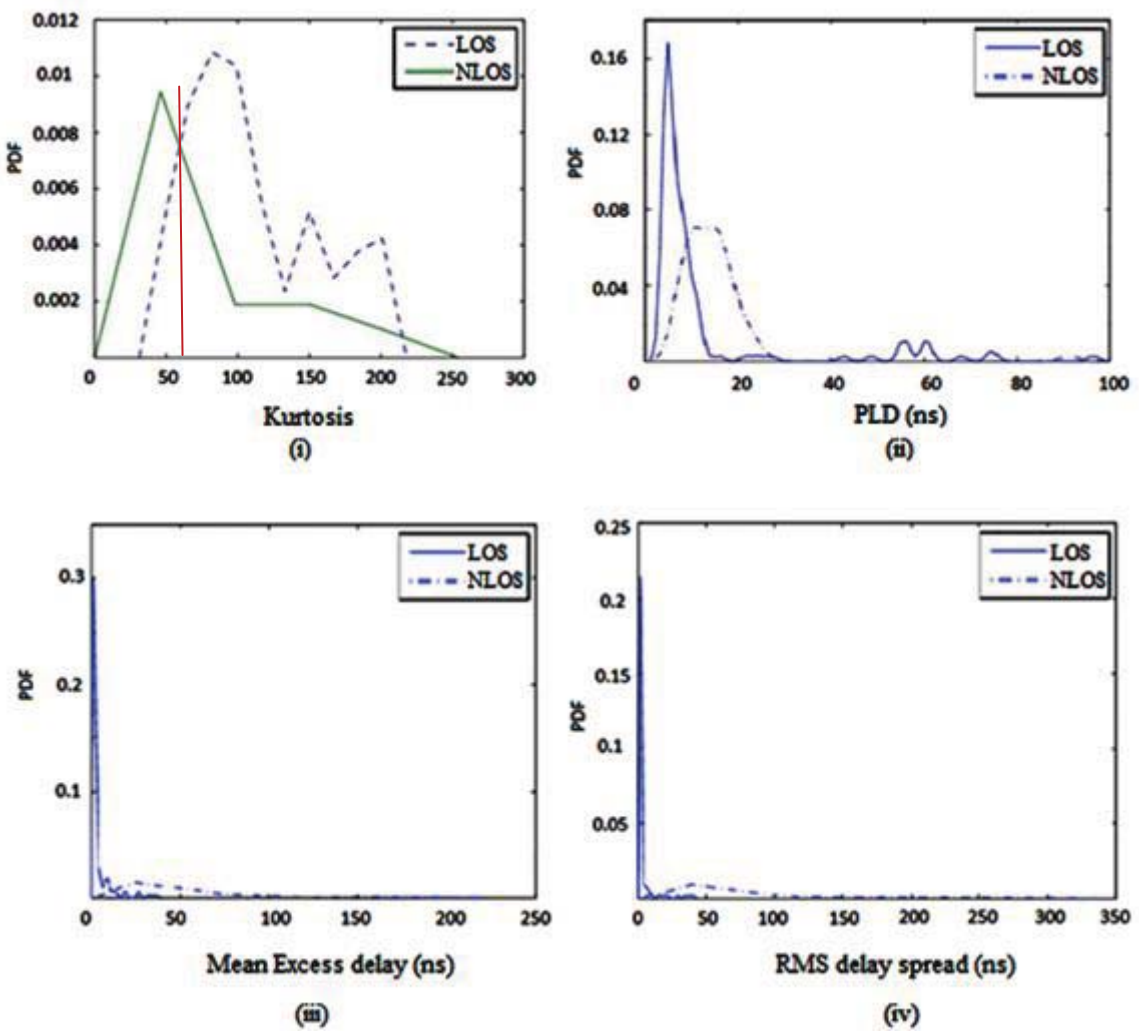

Figure 3.15: PDF of (i) Kurtosis, (ii) Peak to Lead delay, (iii) Mean Excess delay, and (iv) RMS delay spread of LOS NLOS scenarios based from measurement data after deconvolution.

Similarly for Mean Excess delay we observe that a threshold of 21 if deployed can distinguish between LOS and NLOS signals. The RMS delay spread, for a particular signal of the measurement data bank, if below 18 would mean that the signal is possibly a LOS. On performing the Likelihood Ratio test, it is found that there is a 5% - 8% increase

in the correctly identified profiles post deconvolution for Kurtosis and PLD, and this percentage increases up to 12% - 15% for Mean Excess delay and RMS delay spread.

A comparison between the LOS and NLOS signals before deconvolution and after deconvolution was done and was found that a reasonable classification is possible if the signals are deconvolved before their Kurtosis, Mean Excess delay, RMS, PLD values are computed and their PDFs evaluated. Figure 3.16 shows a plot to support this discussion. Figure 3.16 (i) is the PDF of the RMS delay spread without deconvolution and Figure 3.16 (ii) is the PDF of the RMS delay spread after deconvolution using Subtractive deconvolution with multi (5) templates and 20 multipaths.

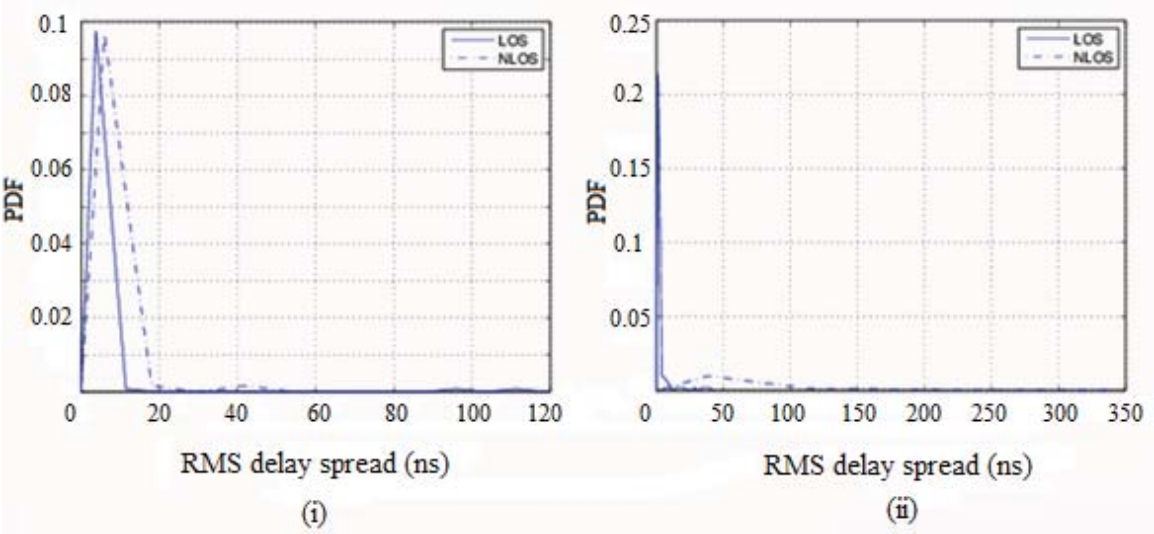

Figure 3.16: PDF of the RMS delay spread of the LOS NLOS measurements

(i) before deconvolution (ii) after deconvolution.

It is observed that deconvolution affects the Mean Excess delay and RMS delay spread to a more extent than it does to the Kurtosis and the PLD. And overall there is an improvement in the percentage of correctly classified profiles. This is supported by the Likelihood Ratio test presented.

The KS test was also applied to these signals from the measurement data bank. This is tabulated in Table 3.5. While Mean Excess delay and RMS delay spread were not so helpful for classification of simulated signals, it was found that these parameters gave good results for experimental signals. The PLD was found to have a similar performance in both cases. Kurtosis was found to perform the worst for experimental data while Mean Excess delay had the best performance.

Parameters	Kurtosis	PLD	Mean Excess delay	RMS delay spread
Measurement Data	0.87	0.32	0.15	0.16

Table 3.5: KS test for the profiles of the measurement data

Likelihood Ratio test results are tabulated in Table 3.6. Results for Kurtosis and PLD for the measured data resemble results of the Residential environment and the Indoor Office environment respectively, of the simulated full profile of the IEEE channel model.

Parameters / Channel	Kurtosis	PLD	Mean Excess delay	RMS delay spread	Kurtosis, PLD & RMS
LOS	68.9	82.7	93.1	97.3	95.6
NLOS	82.1	73.9	92.5	94.8	96.3

Table 3.6: LOS/NLOS identification percentages for measurements post deconvolution.

3.6.4 Impact of Subsetting on Performance of Parametric Analysis

Processing of the entire channel profile can be time consuming when the number of profiles considered is huge. There is a tradeoff between complexity, processing time and performance. Thus, a suboptimal approach is required that reduces processing time but maintains the performance above a certain satisfactory level. To achieve this, we propose a new method which is to process a partial representation of the channel profile instead of using the entire received profile. The profile is subsetted at local cluster peaks wherein only 5, 10 or 20 paths are selected from the profile to evaluate parameters like Kurtosis, PLD, Mean Excess delay, RMS delay spread. It is found that based on this subsetted version, we still can make a successful classification between LOS/NLOS signals.

The ways in which the few paths are selected from the received profile also make a difference in ease of identification between LOS/NLOS scenarios. For each of the cases mentioned in 3.3, the normalized histograms were plotted to test the effect of initial sample selection, spread sample selection and local cluster peaks selection.

The selection of paths from cluster heads of the local peaks is found to be the best method of paths selection among the three discussed methods. It is found to present the maximum difference in the obtained PDFs. Also it bears most resemblance with the case where the entire channel profile is considered. This is also in accordance with the reference paper [Guv07] that deals with NLOS identification and mitigation for UWB localization systems.

In Figure 3.17 a plot of the PDF of the Kurtosis of CM1 & CM2 for 20 paths is presented. Cluster head-based subsetting provides the best distinction between

LOS/NLOS signals and bears closest resemblance to the reference full profile. Figure 3.18 depicts a plot of the PDFs of Mean Excess delay for CM3 (LOS) & CM4 (NLOS) with 20 paths for the three ways of paths selection along with the reference plot for the full profile. From these figure we observe that when the paths are selected from the local cluster heads we have a better identification chance compared to the other two methods.

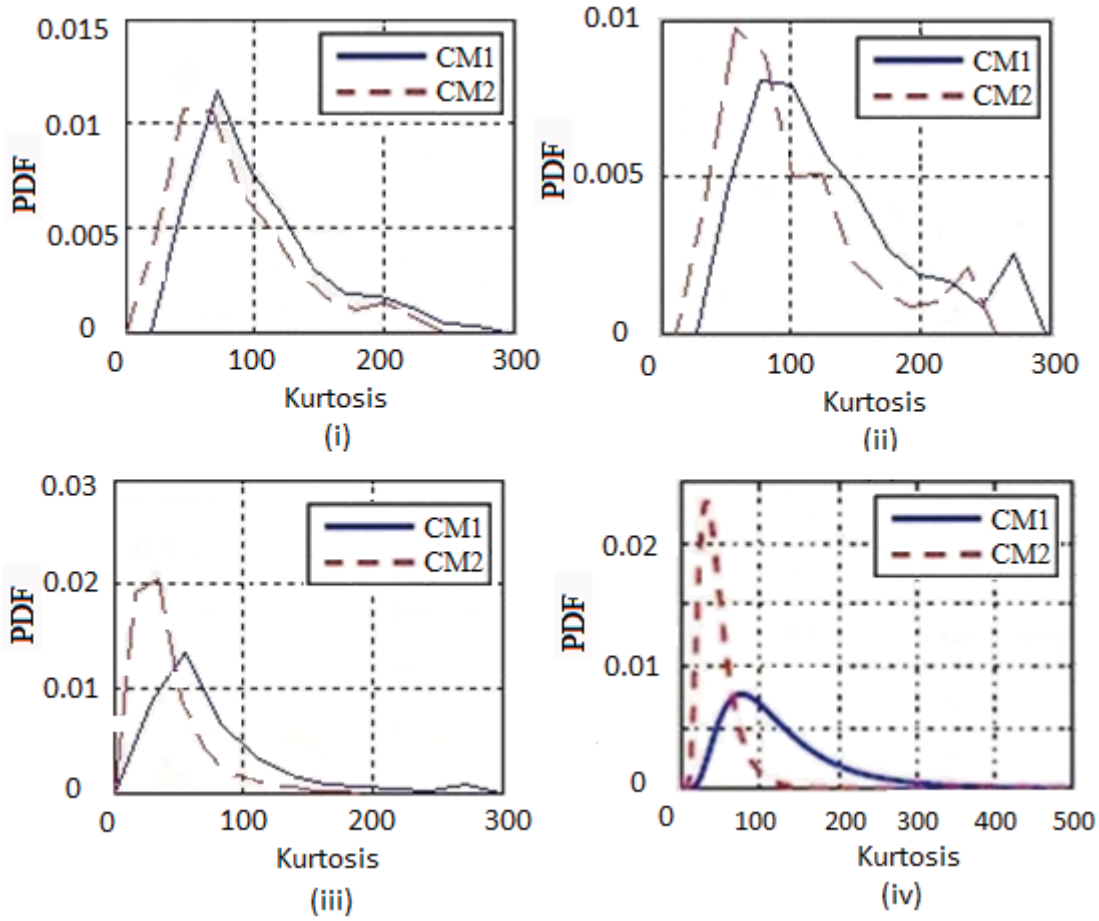

Figure 3.17: PDFs of Kurtosis of CM1 (LOS) & CM2 (NLOS) with just 20 paths for cases (i) Initial samples, (ii) Spread samples (iii) Cluster Head samples (iv) Full Profile [Guv07].

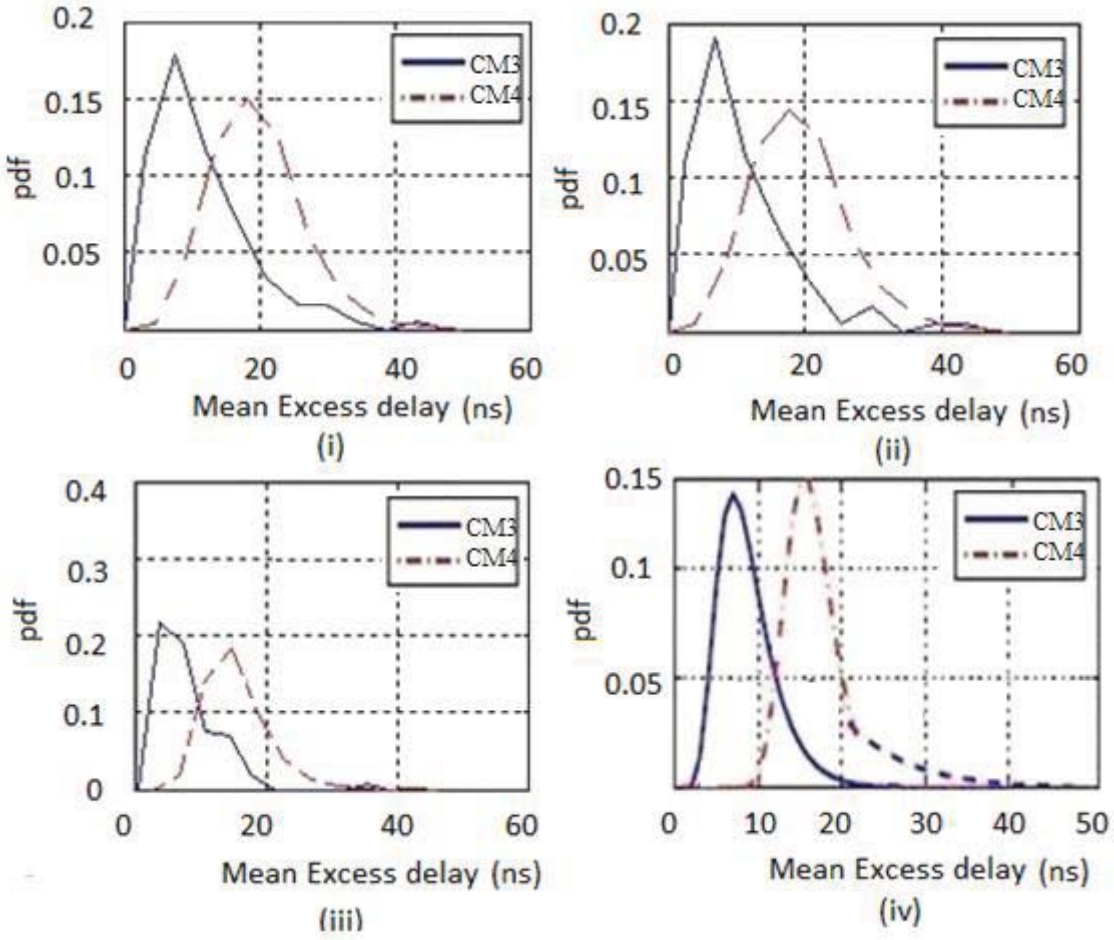

Figure 3.18: PDFs of Mean Excess delay of CM3 (LOS) & CM4 (NLOS) with just 20 paths for cases (i) Initial samples, (ii) Spread samples (iii) Cluster Head samples (iv) Full Profile [Guv07].

The PDFs of RMS delay spread for CM1 & CM2 and CM5 & CM6 are plotted respectively in comparison with the PDFs plotted for the full profiles, by the reference paper in Figure 3.19. The PDFs generated are found to bear close resemblance. They were plotted by selecting local peak heads as sample paths.

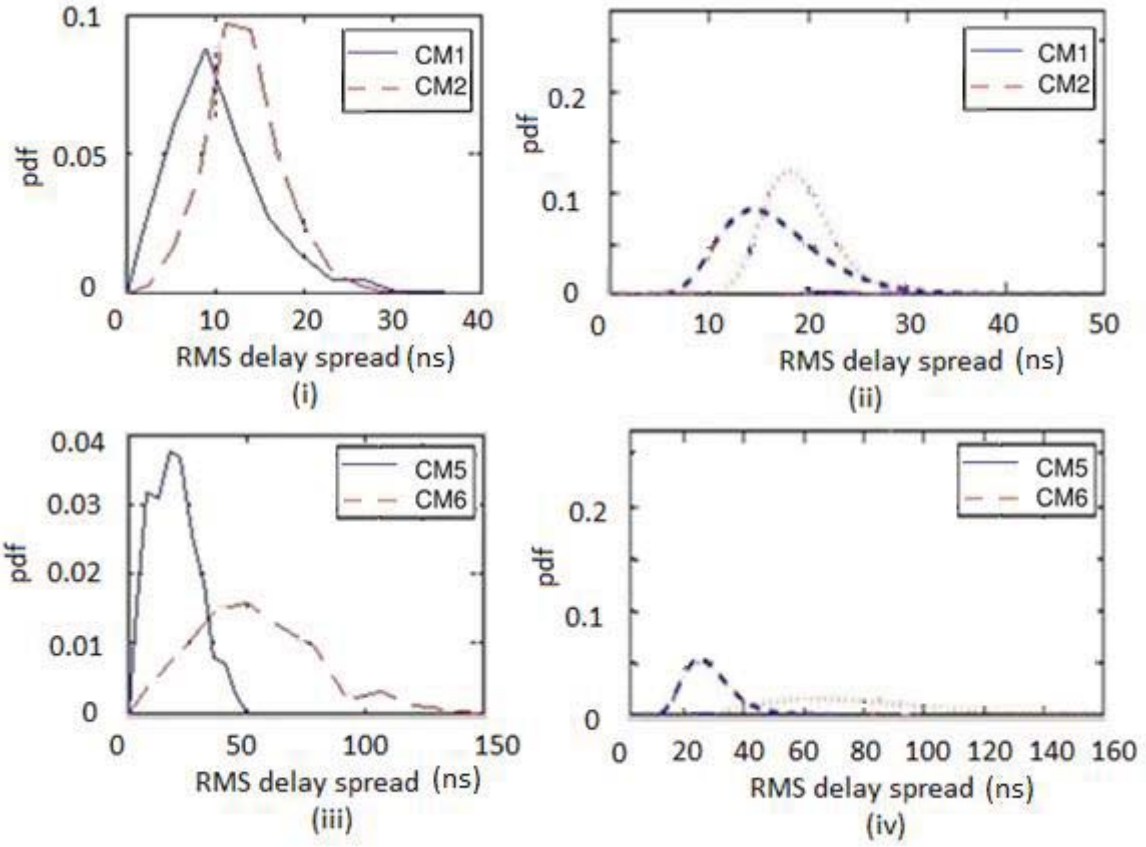

Figure 3.19: PDFs of RMS Delay Spread of CM1 (LOS) / CM2 (NLOS) with 20 paths for cases (i) Cluster Heads Samples (ii) Full Profile [Guv07] & CM5 (LOS) / CM6 (NLOS) with just 20 paths for cases (iii) Cluster Heads Samples (iv) Full Profile [Guv07].

Since selection of cluster heads was found to be the best way to subset the channel profile, it was further implemented for all channel environments of the channel model.

Figure 3.20 shows a plot of the PDF of the Kurtosis for the channel model with cluster head-based subsetted profile paths for all LOS/NLOS scenarios. It is observed that these paths can be used efficiently to make an identification except for the case of outdoor environment.

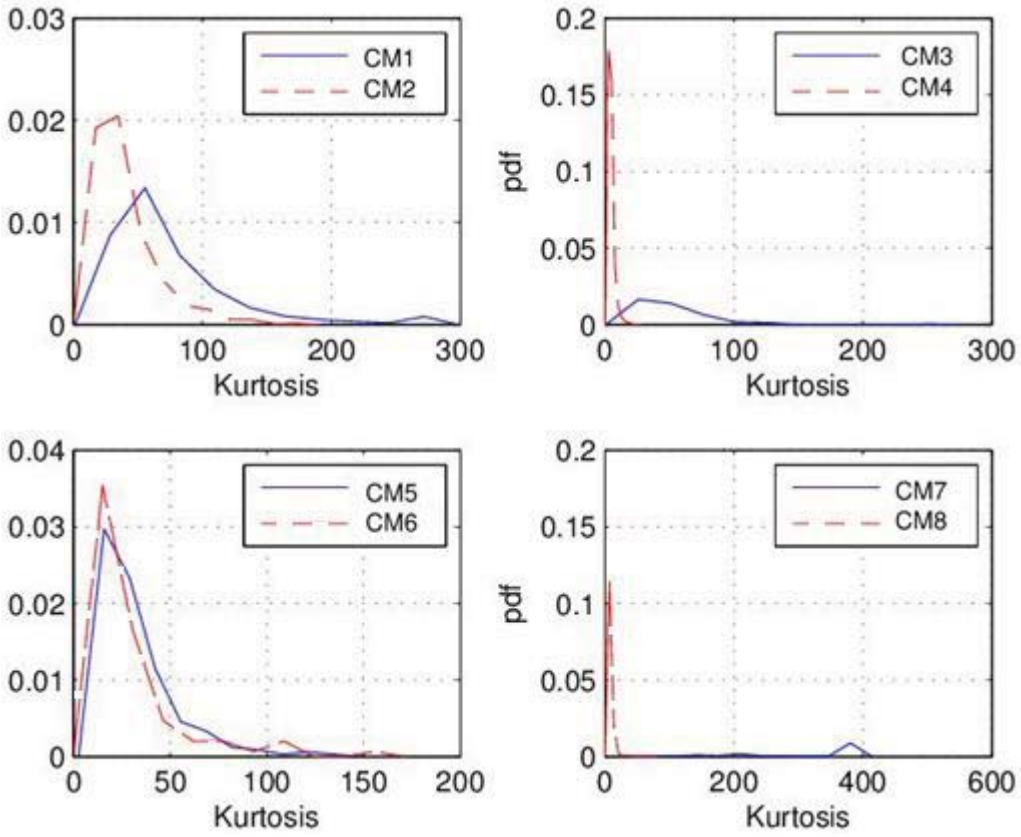

Figure 3.20: PDFs of Kurtosis of cluster head-based subsetted channel models.

The PLD for this subsetted profile is also calculated and is plotted in Figure 3.21. It is observed here also that LOS signals have lower PLDs compared to NLOS signals except for the case of CM7 and CM8.

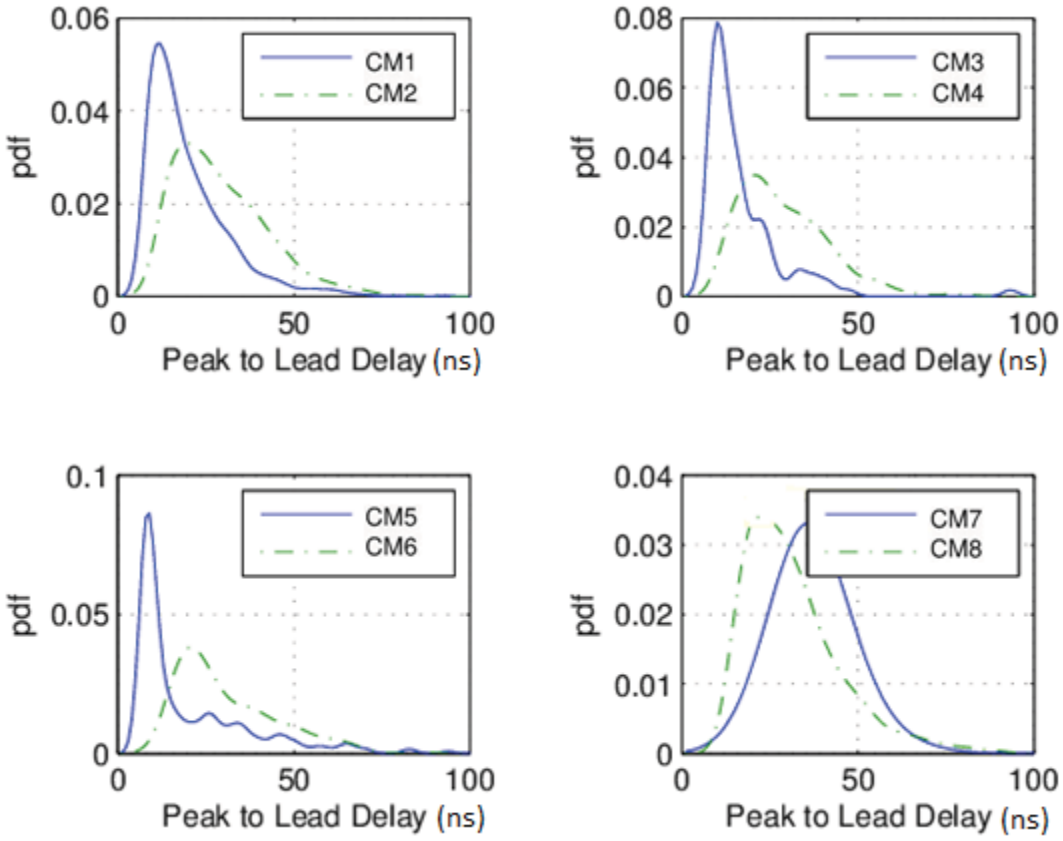

Figure 3.21: PDFs of PLD of cluster head-based subsetted channel models.

Similar to the Kurtosis and PLD, the Mean Excess delay is also evaluated for the subsetted channel profile. This is presented in Figure 3.22 and is observed from the plot that apart from indoor Residential scenario (CM1/CM2) all other scenarios provide a good identification plot.

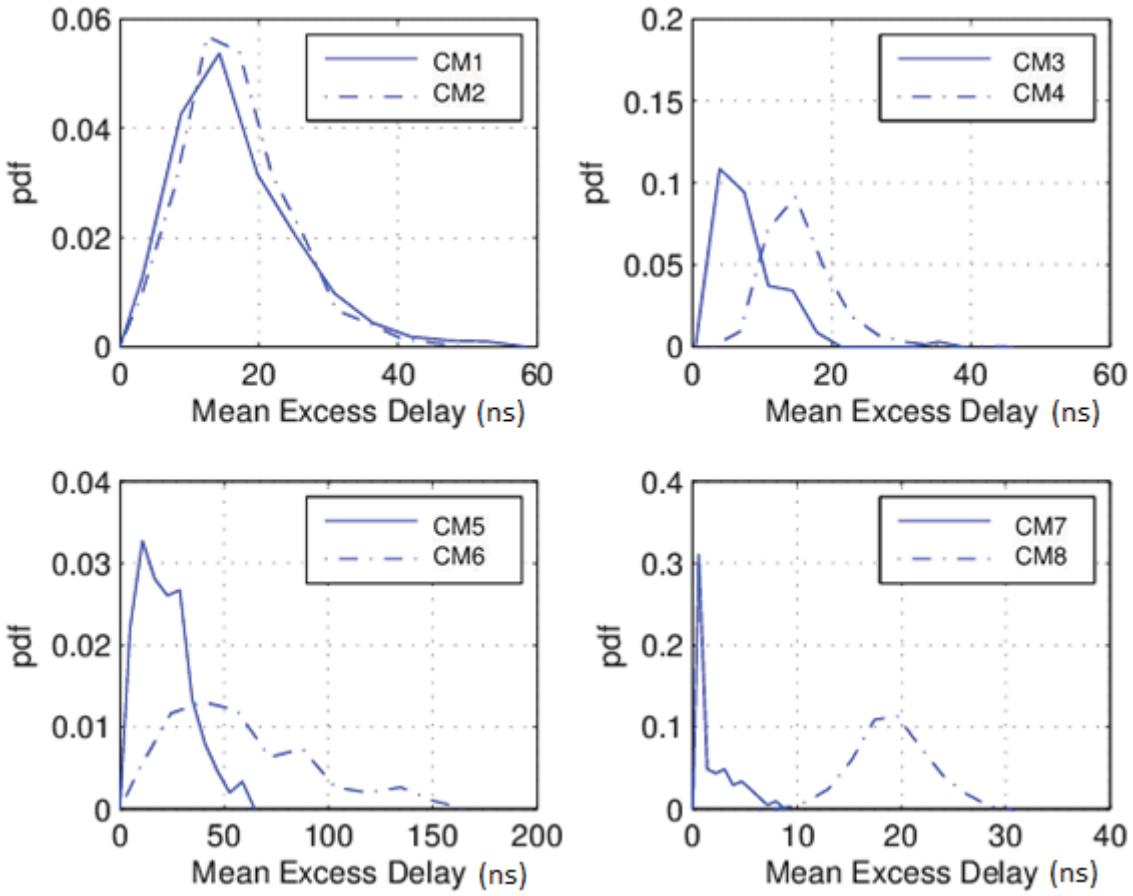

Figure 3.22: PDFs of Mean Excess delay of cluster head-based subsetted channel models.

RMS delay spread for all scenarios of the cluster head-based subsetted channel model is plotted and presented in Figure 3.23.

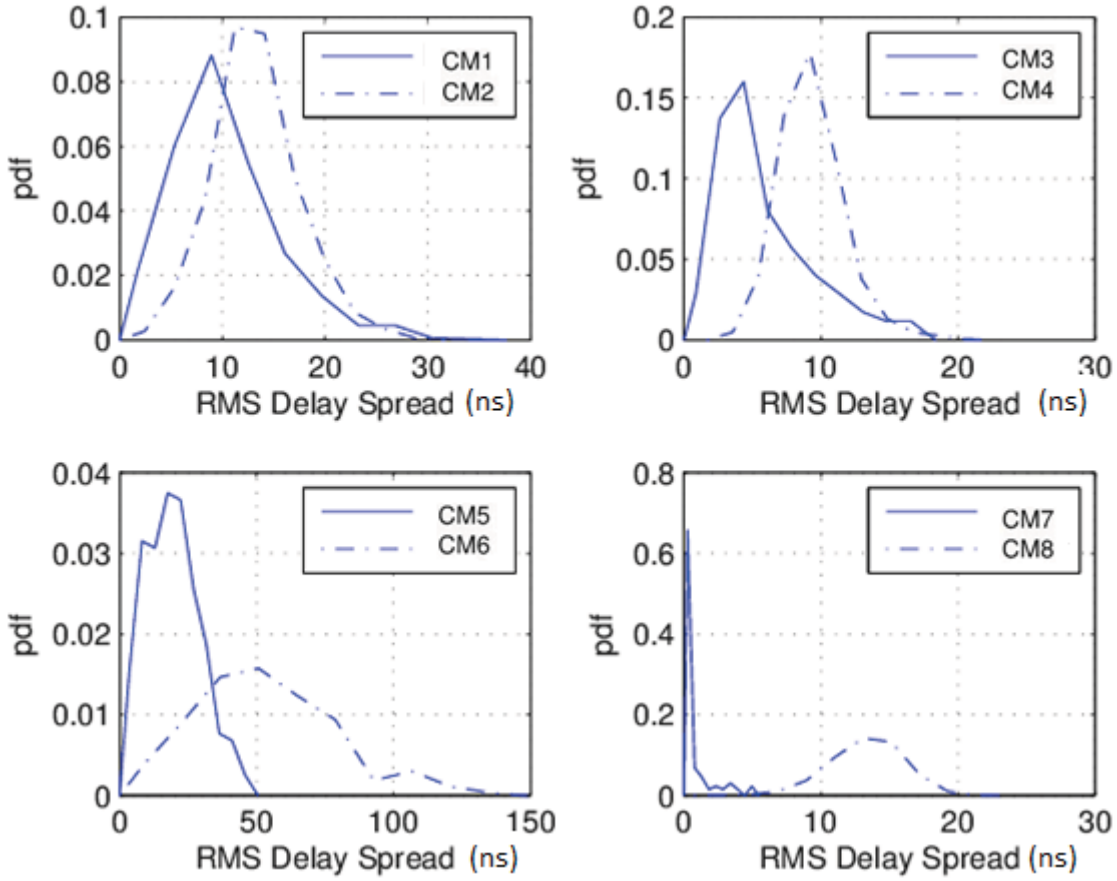

Figure 3.23: PDFs of RMS delay spread of cluster head-based subsetted channel models.

It is evident from the obtained results that using a cluster head-based subsetted version of the channel profile is an efficient way to reduce processing time while retaining a good classification capability.

The probability/likelihood of the subsetted IEEE channel profile to be correctly identified is evaluated using the Likelihood Ratio test. The performance was found to decline by a small percentage for the individual parameters, compared to the full profile, but the joint hypothesis provided a good result with a minimum correct identification percent of 85% for the profiles. This is presented in Table 3.7.

Parameters / Channel	Kurtosis	PLD	RMS	Kurtosis & PLD	Kurtosis & RMS	PLD & RMS	Kurtosis, PLD, RMS
CM1 (LOS)	66.7	63.4	56.9	84.5	77.3	79.3	87.7
CM2 (NLOS)	73.1	61.0	79.5	86.0	89.4	79.1	89.7
CM3 (LOS)	80.8	74.0	67.0	88.2	100	86.0	87.3
CM4 (NLOS)	88.1	66.6	93.6	88.8	99.2	91.0	93.1
CM5 (LOS)	61.2	79.6	92.0	88.4	85.2	88.4	89.2
CM6 (NLOS)	54.2	70.0	79.4	81.5	84.2	76.3	85.1
CM7 (LOS)	88.4	92.8	99.4	91.9	96.8	98.8	96.9
CM8 (NLOS)	89.7	92.6	99.7	90.9	90.3	98.6	97.4

Table 3.7: LOS/NLOS identification percentages for subsetted IEEE channel model.

Similar to the case of the full profile, Kurtosis performed well for all environments except to CM5/CM6 while RMS delay spread had lower identification percentages for CM1 and CM3. PLD was again found to perform consistently moderate compared to the two parameters, irrespective of the environment. The joint optimization technique involving Kurtosis, PLD and RMS delay spread was found to be effective for the subsetted channel profiles too.

From our observations, we conclude that the hybrid technique of using Kurtosis, PLD and RMS delay spread for channel classification is a promising approach in UWB systems.

This chapter focused on evaluation of the various channel parameters for classification of both simulated environment and measurement data. The Two sample KS test and the Likelihood Ratio test were applied to numerically support the work.

The impact of thresholding was also studied and it was found that signals thresholded for noise removal provide better classification.

The deconvolution technique applied improved the percentage of correctly identified LOS/NLOS signals by 5% for PLD and by 8% for Kurtosis, post deconvolution. While Mean square delay and RMS delay were improved by approximately 15%.

Subsetted version of the simulated IEEE model, obtained by selecting the cluster heads within the signal, was also explored and found to be quite effective in LOS/NLOS classification. While it reduces processing time by a great amount a small degradation in the overall performance, of the order of just 2% in most scenarios of the IEEE channel model, was observed during the Likelihood ratio test.

Based on the investigation carried and the results obtained, a hybrid (improved) technique for channel identification was introduced. This method guaranteed a minimum of 90% correct identification percentage under the Likelihood ratio test, which is closed to 10% better than that obtained for some of the individual parameters.

Chapter4

CONCLUSION & FUTURE WORK

This chapter provides a summary of the work accomplished and some suggestions for future work.

4.1 Summary of Contributions

The two main topics investigated in this work are the TOA estimation based on the Unscented Kalman Filter-based approach and the parametric approach for LOS/NLOS classification of UWB signals by examining the CIR and evaluating the parameters: Kurtosis, Peak to Lead delay, Mean Excess delay, RMS delay spread.

Under the UKF module work was done for TOA estimation with varying SNRs in Nakagami environments with varying Nakagami parameters. The performance of the algorithm was found to be directly related to the SNR maintained, i.e., higher SNR assured better performance; while changing the Nakagami factor had no significant change in the performance. The algorithm was tested for 4 and 8 paths and found to be converging for both cases. Also, the TOA of the first path was estimated by varying SNRs, Nakagami fading environments and varying path spaces between the multipath signals, where the error in estimation was found to have a Gaussian behavior irrespective

of the fading environment. A decrease in the SNR by half; approximately doubled the variance of the Gaussian error.

Under the parametric approach the channel parameters mentioned earlier were evaluated for classification of both simulated environment and measurement data. Also evaluation measures such as the KS test and the Likelihood Ratio test were applied to check the percentage of correct identification of channels.

The difference in dealing with experimental results compared to simulated data was observed. While the Mean Excess delay and the RMS delay spread were found to be less effective in LOS/NLOS classification for the Indoor scenarios of simulated data, they were efficient in providing classification information for experimental measurements taken indoors. The impact of thresholding was also studied and it was found that signals thresholded for noise removal provide better classification.

In order to extract the channel impulse response from the received signal a deconvolution technique was employed which improved the percentage of correctly identified LOS/NLOS signals. The PLD identification was found to improve by 5% and the Kurtosis by 8% post deconvolution. While Mean square delay and RMS delay were improved by approximately 15%.

Subsetted version of the simulated IEEE model, obtained by selecting the cluster heads within the signal, was also explored and found to be quite effective in LOS/NLOS classification. While it reduces processing time by a great amount a small degradation in the overall performance, of the order of just 2% in most scenarios of the IEEE channel model, was observed during the Likelihood ratio test.

Based on the investigation carried and the results obtained, a hybrid (improved) technique for channel identification which was the selection of a joint estimation scheme involving Kurtosis, PLD and RMS delay spread was suggested and justified. This method guaranteed a minimum of 90% correct identification percentage under the Likelihood ratio test, which is closed to 10% better than that obtained for some of the individual parameters.

4.2 Future Work

This work helps in better time estimation and channel identification, the next step would be to study the impact of this estimation and identification in positioning estimation. Work in this direction is being done as part of a Master Thesis.

The power of the paths of the received signal in the UKF-based approach was exponentially generated in this work. Other distributions such as the lognormal can be investigated.

A possible direction in extending the parametric approach is to explore the performance of new parameters, and, their ability to assist in LOS/NLOS classification can be analyzed. Based on the classification obtained a NLOS mitigation technique, for ex: Weighted Least Square can be implemented.

For eliminating the unwanted noise in our received signals we did a preliminary study and found delay independent thresholding scheme suitable for our work; delay dependent thresholding can be deployed to test the performance.

After deconvolution the estimated channel impulse response is independent of the excitation signal. Thus, the effect of different pulse shapes can be studied.

Two evaluation measures, the KS Test and the Likelihood Ratio test, were carried out in this work, other test for example the Cramér-von-Mises test could be conducted.

Also, the hybrid technique used in our work had the assumption that the parameters are independent of each other. The dependence between these parameters can be investigated.

NOMENCLATURE

List of Abbreviations

AOA	Angle of Arrival
APDP	Average Power Delay Profile
AWGN	Additive White Gaussian Noise
CIR	Channel Impulse Response
CM	Channel Model
DD	Delay dependent
DI	Delay independent
ED	Energy Detector
EKF	Extended KF
GML	Generalized-ML
IR	Impulse Radio
KF	Kalman filter
KS	Kolmogorov Smirnov
LOS	Line of Sight

MF	Matched Filter
ML	Maximum Likelihood
MMSE	Minimum Mean-Square Error
MPCs	Multipath Components
MSE	Mean-Square Error
NLOS	Non Line of Sight
PDP	Power Delay Profile
PLD	Peak to Lead delay
RMS	Root Mean Square
RSS	Received Signal Strength
SNR	Signal to Noise Ratio
TDOA	Time Difference of Arrival
TNR	Threshold to Noise Ratio
TOA	Time of Arrival
UKF	Unscented Kalman Filtering
UWB	Ultra Wideband

List of Symbols

a	spreading waveform
$a_{k,l}^{i}$	multipath gain coefficient
$c_i(l)$	channel coefficient
$d_{k,m}$	data bits
$d_{m(l)}$	m^{th} symbol transmitted
$E[\ ]$	Expected value
F_c & F_τ	state transition matrices of UKF Algorithm
$h(t)$	channel impulse response
K	total number of paths within a cluster
k	Kurtosis
L	total number of clusters
m, μ	Nakagami factor
$n(l)$	AWGN
$P(\tau)$	PDP
Q	noise covariance matrix
q	number of samples per chip

T_b	symbol interval
T_c	chip duration
T_l	time arrival of the first path of the first cluster
T_l^i	delay of l^{th} cluster
t	time (in nano seconds)
$v_c(l)$ & $v_\tau(l)$	mutually independent Gaussian random variable s for amplitude and delays resp.
$W_i^{(m)}$ & $W_i^{(c)}$	UKF weights for mean and covariance respectively.
X_i	lognormal shadowing where the subscript i refers to the i^{th} realization
x	Gaussian random variable
α	controls the spread of the sigma points
β	incorporates the prior knowledge of the distribution of 'x'
β	mixture probability (in IEEE channel model)
γ_l	intra-cluster decay time constant
κ	kappa, secondary scaling parameter
λ_1 , λ_2	ray arrival rates
$\mu_{\lvert h \rvert}$	mean of $h(t)$

$\sigma_n^{\,2}$	noise covariance
$\tau_i(l)$	*time delay*
$\tau_{k,l}$	delay of the k^{th} path in the l^{th} cluster relative to T_l
$\tau_{k,l}^{i}$	delay of the k^{th} multipath component relative to the l^{th} cluster-arrival time
τ_{med}	Mean Excess delay
τ_{pld}	Peak to Lead delay
τ_{rms}	RMS delay spread

REFERENCES

[Ali09] Z. A. Khan, M. A. Landolsi, and M. Deriche, "Multipath Channel Estimation for CDMA Signals using The Unscented Kalman Filter", *International Journal of Ultra Wideband Communications and Systems*, vol.1, no. 2, pp. 151-158, 2009.

[And02a] C. R. Anderson, T. S. Rappaport, K. Bae, A. Verstak, N. Ramakrishnan, W. Tranter, C. Shaffer, and L. Watson, "In-Building Wideband Multipath Characteristics at 2.5 & 60 GHz", *Proceedings of IEEE 56th Vehicular Technology Conference*, vol.1, pp. 97-101, 2002.

[And02b] C. R. Anderson, *Design and Implementation of an Ultrabroadband Millimeter-Wavelength Vector Sliding Correlator Channel Sounder and In- Building Multipath Measurements at 2.5 & 60 GHz*, Thesis Submitted to the Faculty of the Virginia Polytechnic Institute and State University, May 2002.

[Ben06] M. G. D. Benedetto, T. Kaiser, A. F. Molisch, I. Oppermann, C. Politano, and D. Porcino, "UWB Communication Systems A Comprehensive Overview", *EURASIP Book Series on Signal Processing and Communications*, vol. 5, pp. 5, 2006.

[Cas02] D. Cassioli, M. Z. Win, and A. F. Molisch, "The ultra-wide bandwidth indoor channel: from statistical model to simulations", *IEEE Journal on Selected Areas in Communications*, vol. 20, no. 6, pp. 1247–1257, 2002.

[Caf00] J.J. Caffery, Jr. and G.L. Stuber, 'Nonlinear multiuser parameter estimation and tracking in CDMA systems', *IEEE Transactions on Communications*, vol. 48, no. 12, pp.2053–2063, Dec. 2000.

[Che05] P. Cheong, A. Rabbachin, J. Montillet, K. Yu, and I. Oppermann, "Synchronization, TOA and position estimation for low-complexity LDR UWB devices", *in Proc. IEEE Int. Conf. on Utra-Wideband (ICU)*, Zurich, Switzerland, pp. 480–484, Sep. 2005.

[Cho05a] C.-C. Chong and S. K. Yong, "A generic statistical-based UWB channel model for high-rise apartments", *IEEE Transactions on Antennas and Propagation*, vol. 53, no. 8, pp. 2389–2399, 2005.

[Cho05b] C.-C. Chong, Y.-E. Kim, S. K. Yong, and S.-S. Lee, "Statistical characterization of the UWB propagation channel in indoor residential environment", *Wireless Communications and Mobile Computing*, vol. 5, no. 5, pp. 503–512, 2005.

[Dar04] D. Dardari, "Pseudo-random active UWB reflectors for accurate ranging", *IEEE Communication Letters*, vol. 8, no. 10, pp. 608–610, 2004.

[Dar06a] D. Dardari, M. Z. Win, "Threshold-based time of- arrival estimators in UWB dense multipath channels", *IEEE International Conference on Communications,* vol.1, 2006. Pages: 4723 -4728, 2006.

[Dar06b] D. Dardari, C.-C. Chong, and M. Z. Win, "Analysis of Threshold-based TOA estimators in UWB channels", *14th European Signal Processing Conference*, Florence, Italy Sep. 2006.

[Dar07] D. Dardari, A. Giorgetti, and M. Z. Win, "Time-of-arrival estimation in the presence of narrow and wide bandwidth interference in UWB channels", *in Proc. IEEE International Conference on Ultra-Wideband, (ICUWB)*, Singapore, vol. 1, pp. 71-76, Sep. 2007.

[Dar08] D. Dardari, C.-C. Chong, and M. Z. Win, "Threshold-based time of-arrival estimators in UWB dense multipath channels", *IEEE Trans. Commun*., vol. 56, pp. 1366-1378, 2008.

[Fal06] C. Falsi, D. Dardari, L. Mucchi, M. Z. Win, "Time of arrival estimation for UWB localizers in realistic environments", *EURASIP J. Applied Signal Processing, Special Issue on Wireless Location Technologies Applications*, vol. 2006, article ID 32082, pp. 1-13, 2006.

[Guv05a] I. Guvenc and Z. Sahinoglu, "Threshold selection for UWB TOA estimation based on Kurtosis analysis", *IEEE Commun. Lett*., vol. 9, no. 12, pp. 1025-1027, Dec. 2005.

[Guv05b] I. Guvenc and Z. Sahinoglu, "Threshold-based TOA estimation for impulse radio UWB systems", *IEEE Int. Conf. UWB (ICU),* pp. 420-425, Sep. 2005.

[Guv06a] I. Guvenc, Z. Sahinoglu, and P. Orlik, "TOA estimation for IR-UWB systems with different transceiver types", *IEEE Trans. Microwave Theory and Techniques (special issue on ultrawideband),* vol. 54, no. 4, pp. 1876–1886, Apr. 2006.

[Guv06b] I. Guvenc and H. Arslan, "Comparison of two searchback schemes for non-coherent TOA estimation in IR-UWB systems", *IEEE Sarnoff Symp.*, Princeton, NJ, Mar. 2006.

[Guv07] I. Guvenc, C. Chong, and F. Watanabe, "NLOS Identification and Mitigation for UWB Localization Systems", *Wireless Communications and Networking Conference, IEEE*, pp. 1571-1576, Mar. 2007.

[Haw91] D. A. Hawbaker, *Indoor wide band radio wave propagation measurements and models at 1.3 GHz and 4.0 GHz,* M.S. thesis, Dep. Elec. Eng., Virginia Polytech. Inst. And State Univ., May 1991.

[Hay01] S. Haykin, "Kalman Filtering and Neural Networks", *John Wiley & Sons. Inc.*, 2001.

[Ian82] J. P. Ianniello, “Time delay estimation via cross-correlation in the presence of large estimation errors”, *IEEE Trans. Acoust., Speech, Signal Processing*, vol. ASSP-30, no. 6, pp. 998–1003, Dec. 1982.

[Jul04] S.J. Julier, and J.K. Uhlmann, ‘Unscented filtering and nonlinear estimation’, *Proceedings of the IEEE*, vol. 92, no. 3, pp.401–422, 2004.

[Kim02] K. J. Kim and R.A. Iltis, ‘Joint detection and channel estimation algorithms for QS-CDMA signals over time varying channels’, *IEEE Transactions on Communications*, vol. 50, no. 5, pp.845–855, 2002.

[Kol10] J. Kolakowski, “A Method for Reduction of TDOA Measurement Error in UWB Leading Edge Detection Receiver”, *Proceedings of the 40th European Microwave Conference*, pp. 1512-1515, Sep. 2010.

[Mol05] A. F. Molish, K. Balakrishnan, C.-C. Chong, S. Emami, A. Fort, J. Karedal, H. Schantz, U. Schuster, K. Siwiak, “IEEE 802.15.4a channel model-final report,” *Tech. Rep.*, *Environments*, vol. 15, pp. 1-40, Sep. 2005.

[Muc09] L. Mucchi and P. Marcocci, “A New Parameter for UWB Indoor Channel Profile Identification”, *IEEE Transactions on Wireless Communications*, vol. 8, No. 4, pp. 1597-1602, Apr. 2009.

[Muq03] A. H. Muqaibel, “*Characterization of Ultra Wideband Communication Channels*”, Thesis Submitted to the Faculty of the Virginia Polytechnic Institute and State University, Mar. 2003.

[Muq06] A. Muqaibel, A. Safaai-Jazi, A. Attiya B. Woerner, and S. Riad, "Pathloss and Time Dispersion Parameters for Indoor UWB propagation", *IEEE Transactions on Wireless Communications,* vol. 5, No. 3, pp. 550-559, Mar. 2006.

[Rab06a] A. Rabbachin, I. Oppermann, and B. Denis, "ML time-of-arrival estimation based on low complexity UWB energy detection", *IEEE Int. Conf. on Utra-Wideband (ICUWB),* Waltham, MA, pp. 599–604, Sep. 2006.

[Rab06b] A. Rabbachin, I. Oppermann, and B. Denis, "GML TOA estimation based on low complexity UWB energy detection", *The 17th Annual IEEE International Symposium on Personal, Indoor and Mobile Radio Communications (PIMRC'06)*, pp. 1-5, Sep. 2006.

[Rap92] T. S. Rappaport and D. A. Hawbaker, "Wide band microwave propagation parameters using circular and linear polarization antennas for indoor wireless channels", *IEEE Trans. Commun.,* vol. 40, no. 2, pp 1-6, Feb. 1992.

[Sei94] S. Sediel, and T. Rappaport, "Site-Specific Propagation Prediction for Wireless In-Building Personal Communication System Design", *IEEE Transactions on Vehicular Technology*, vol. 43, no. 4, pp. 879-891, Nov. 1994.

[Sey05] J. S. Seybold, “Introduction to RF propagation”, John Wiley & sons, Inc., pp. 194, 2005.

[Sha10] F. Shang, B. Champagne and I. Psaromiligkos, “Joint Estimation of Time of Arrival and Power Profile for UWB Localization”, *International Conference on Signal Processing Proceedings*, 1484-1487, Oct. 2010.

[She10a] G. Shen, R. Zetik, H. Yan, O. Hirsch and R. S. Thoma, “Time of Arrival Estimation for Range-Based Localization in UWB Sensor Networks”, *Proccedings of IEEE International Conference on Ultra-Wideband*, pp. 1-4, Sep. 2010.

[She10b] B. Shen, R. Yang, S. Ullah and K. Kwak, “Linear quadrature optimization non-coherent time of arrival estimation scheme for impulse radio ultra-wideband systems”, *IET Communications*, vol. 4, issue 12, pp. 1471–1483, Aug. 2010.

[Van10] F. Van, Y. L. Guan and M. Moeneclaey, ‘Optimal Channel and Time of Arrival Estimation for IR-UWB in the presence of pulse overlap”, *International Conference on Communications proceedings*, *IEEE*, pp. 1-5, May 2010.

[Win98] M. Z. Win and R. A. Scholtz, "On the robustness of ultra-wide bandwidth signals in dense multipath environments", *IEEE Communications Letters*, vol. 2, no. 2, pp. 51–53, Feb. 1998.

[Win00] M. Z. Win and R. A. Scholtz, "Ultra-wide bandwidth time hopping spread-spectrum impulse radio for wireless multiple access communications", *IEEE Transactions on Communications,* vol. 48, no. 4, pp. 679–689, Apr. 2000.

[Xu08] Y. Xu, E, K. S. Au, A. K. Wong and Q. Wang, "Time of Arrival Estimation for IR-UWB Systems in Dense Multipath Environment", *IEEE*, pp. 1-5, Sep. 2008.

[Yu04] K. Yu and I. Oppermann, "Performance of UWB position estimation-based on time of arrival measurements", *in Proceedings of International Workshop on Ultra Wideband Systems; Joint with Conference on Ultrawideband Systems and Technologies (Joint UWBST & IWUWBS '04),* pp. 400–404, Kyoto, Japan, May 2004.

[Yu09] Xu Yubin, Jiang Weilin, Sha Xuejun, "TOA Estimate Algorithm-based UWB Location", *International Forum on Information Technology and Applications*, pp. 249-252, May 2009.

[Zha04] J. Zhang, R. A. Kennedy, and T. D. Abhayapala, "Cramer-Rao lower bounds for the time delay estimation of UWB signals", *in Proc. IEEE Int. Conf. on Commun.*, Paris, France, vol. 6, pp. 3424–3428 , May 2004.

[Zha08] R. Zhang, X. Dong, "A New Time of Arrival Estimation Method Using UWB Dual Pulse Signals", *IEEE Transactions on Wireless Communications*, vol.7, no.6, June 2008.

[Zha10] H. Zhan, J.Y. L. Boudec, J. Ayadi and J. Farserotu, "Theoretical Limit of Impulse Radio Ultra-WideBand TOA Positioning and TDOA Positioning", *International Conference on Communications proceedings*, *IEEE*, pp. 1-6, May 2010.

VITA

Mohammed Naseeruddin Mahmood was born in 1986 in Hyderabad, India.

He received his Bachelor of Engineering (BE) with distinction in Electronics and Communication Engineering from Osmania University, Hyderabad, India, 2008.

He joined Electrical Engineering Department at King Fahd University of Petroleum and Minerals (KFUPM), Dhahran, Saudi Arabia, as Research Assistant and Masters Student. In June 2011 he completed his Masters Degree in Telecommunication Engineering (M.S.T.E) under the Electrical Engineering at KFUPM.

During his Masters program he has published:

- Asrar U. H. Sheikh and M. Naseeruddin Mahmood, "Channel Sounding in Corridors of an Academic Building", *Proceedings of the 7th international conference on Information, communications and signal processing*, pp.1330-1333, Dec. 2009.

He can be contacted via email at:

- naseer@kfupm.edu.sa